Submitted to *INFORMS Journal on Computing*
manuscript (Please, provide the manuscript number!)

Decomposing loosely coupled mixed-integer programs for optimal microgrid design

Alexander J. Zolan
Thermal Systems Group, National Renewable Energy Laboratory, Golden, CO 80401, alexander.zolan@nrel.gov

Michael S. Scioletti
Department of Mathematical Sciences, United States Military Academy, West Point, NY 10996, michael.scioletti@usma.edu

David P. Morton
Department of Industrial Engineering and Management Sciences, Northwestern University, Evanston, IL 60208, david.morton@northwestern.edu

Alexandra M. Newman
Department of Mechanical Engineering, Colorado School of Mines, Golden, CO 80401, anewman@mines.edu

Microgrids are frequently employed in remote regions, in part because access to a larger electric grid is impossible, difficult, or compromises reliability and independence. While small microgrids often employ spot generation, in which a diesel generator is attached directly to a load, microgrids that combine these individual loads and augment generators with photovoltaic cells and batteries as a distributed energy system are emerging as a safer, less costly alternative. We present a model that seeks the minimum-cost microgrid design and ideal dispatched power to support a small remote site for one year with hourly fidelity under a detailed battery model; this mixed-integer nonlinear program (MINLP) is intractable with commercial solvers, but loosely coupled with respect to time. A mixed-integer linear program (MIP) approximates the model, and a partitioning scheme linearizes the bilinear terms. We introduce a novel policy for loosely coupled MIPs in which the system reverts to equivalent conditions at regular time intervals; this separates the problem into subproblems that we solve in parallel. We obtain solutions within 5% of optimality in at most six minutes across 14 MIP instances from the literature, and solutions within 5% of optimality to the MINLP instances within 20 minutes.

Key words: Mixed-integer Programming; Decomposition; Microgrid, Design and Dispatch

1. Introduction and Literature Review

Spot generation is necessary for remote sites at which electric power must be produced without a connection to the grid, e.g., to administer disaster relief, to maintain quality of life on Native American reservations, to run mines, or to sustain military combat operations. In many cases, each load is satisfied by an individual diesel generator, and requires a rated capacity slightly greater than the designed peak demand for that load source. As a result, total system efficiency is low in off-peak periods, and estimates of the fully burdened cost of fuel can reach \$1,000/gallon when the fuel is transported by air and armored convoy (Erwin 2010). Microgrids that integrate renewable technologies, such as photovoltaic (PV) systems, energy storage technologies (e.g., batteries), and diesel generators, are emerging as a means to power remote sites. Like spot generation, microgrid technology can provide energy needs, but may include PV and battery modules to limit the use of diesel generators and increase efficiency. The fuel consumed by a remote site using these technologies, compared to that by a spot generation strategy, may reduce (i) the required flow of resupply fuel by ground convoys or helicopters, (ii) the environmental footprint, and (iii) wear and tear on the diesel generators, among other benefits.

The availability of portable generation technologies at a remote site limits the design to one or more diesel generators and batteries of various sizes, as well as a modular PV systems in prespecified capacity increments. The costs of design and dispatch include (i) generator, PV system, and battery procurement, (ii) diesel fuel consumption, and (iii) generator and battery "lifecycles," our measurement of the degradation associated with their use. The design decision specifies the number and types of generators, PV systems, and batteries in the microgrid. Dispatch decisions for each time period include which generators to turn on, the power output of all generators and PV systems, and power allocated to charging or discharging the batteries; for this small, non-market-driven environment, we do not make "commitment decisions" typical of large, grid-connected power plants.

In our model, decisions are subject to the following sets of constraints: (i) the design must meet load and spinning reserve requirements for each time period; (ii) power input and output from dispatched generators and batteries are limited by their minimum and maximum rated capacities; (iii) the fuel consumed is a known linear function of each generator's power output and state (on or off) in each time period; (iv) battery power input and output is the (bilinear) product of its voltage and the current into and out of

the battery, respectively, where voltage is a function of the state-of-charge and direction of current; (v) a battery's state-of-charge is a function of that of the previous time period and the net current in the present time period, and is modeled as a percentage of total capacity; (vi) PV systems have a maximum power output per unit for each time period; and, (vii) spatial constraints limit the number of units in the design for each type of PV system. This paper presents a model that seeks to design and dispatch such a microgrid to support a remote site at minimum cost, given known load and PV power output per array at hourly fidelity for an operating time horizon of one year. We refer to this model as the microgrid design and dispatch problem.

The relevant literature includes work to assess microgrid operation policies in which batteries and photovoltaics are modeled as distributed energy resources (e.g., van der Kam and van Sark 2015, Zhang et al. 2016). However, we assume that the area of operation for the microgrid is the size of a football field, obviating the need to enforce alternating current power flow requirements, nor do we account for line losses that would be present in a larger system. The selected set of generators, batteries, and photovoltaics meets alternating current power demand, where: (i) generators are connected directly to an alternating current bus; (ii) batteries are connected to the same bus via bi-directional converters that account for efficiency; and, (iii) the photovoltaics are modeled using a PVWatts calculator (Dobos 2013) that includes seasonal variations and assumes a direct current-to-alternating current conversion and maximum power point tracking. Holding a spinning reserve mitigates the intermittent nature of the photovoltaics; our model requires that a fraction of the photovoltaic power be covered, if necessary, through battery or generator operation. We treat the load as deterministic though our techniques extend to a stochastic environment.

Most microgrid design and dispatch models in the literature enforce nonlinear relationships but restrict operation to a fixed number of potential dispatch strategies, and simulate operations for one or more load scenarios to estimate the total cost. Because enumerating all designs is intractable for realistic instances, these models are solved by heuristic search methods, which use, e.g., a simulation procedure to determine whether a design can meet load under prespecified dispatch rules. Simulation, or a rule-based heuristic, is used to dispatch assets to satisfy demand, in part because nonlinear relationships associated with modeling the incumbent technologies can render problem instances intractable. These

approaches set operating rules, pre-qualify technology procurements, or use site-specific data to obtain a microgrid solution that attempts to meet demand at minimum cost.

Green and Manwell (1995) solve a design and dispatch problem with PV, wind, battery, and diesel generators as candidate technologies by using a time series model to generate scenarios and running a collection of fixed dispatch schemes for potential designs. Barley and Winn (1996) evaluate a set of operations strategies for PV-diesel-battery systems that cycle the batteries to different depths of discharge. The Hybrid Optimization Model for Electric Renewables, or HOMER (Lambert et al. 2005, Bahramara et al. 2016), enumerates a series of dispatch strategies for a user-directed collection of designs. Dufo-López and Bernal-Agustín (2005) use a genetic algorithm to design a PV-diesel system by implementing a collection of operations policies borrowed from HOMER and from Barley and Winn (1996). Katsigiannis and Georgilakis (2008) employ tabu search to size small, isolated hybrid power systems using cycle-charging dispatch, which considers combinations of hybrid system technologies. Bala and Siddiqui (2009) propose to design a PV-diesel hybrid system using genetic algorithms that find a dispatch strategy to minimize net present cost. Gupta et al. (2011) develop a dispatch algorithm to maintain a constant power level for diesel generators in a hybrid system, to maximize the use of renewable technologies. While these approaches yield practical, low-cost designs, they lack proof of (near-) optimality.

Most exact solution methods for optimizing microgrid design and dispatch arise via a MINLP or MIP model, and are limited in time horizon or other model fidelity. Morais et al. (2010) present a MIP for the optimal design of a hybrid system grid, which considers fuel cells and wind power technologies and solves 24-hour instances with hourly fidelity. Huneke et al. (2012) and Barbier et al. (2014) present solutions to year-long instances with hourly fidelity; the former use linear programming to design a microgrid, and the latter optimize the design and dispatch strategy of a system with wind turbines, batteries, and generators via a MIP. Khodaei et al. (2015) present a MIP that optimizes the design and dispatch of a microgrid with generic dispatchable and non-dispatchable assets and energy storage, at hourly fidelity, for at least a year of operation, with linear operating constraints; the authors assume the microgrid is disconnected from the grid for less than one day per year. Huneke et al. (2012), Barbier et al. (2014), and Khodaei et al. (2015) use battery operating constraints similar to those of Barley and Winn (1996), which do not address the variable capacity and degradation of the battery.

Optimization models that include both design and dispatch and integrate hybrid technologies such as batteries, diesel generators, and PV systems are often presented as MINLPs, which are typically intractable for large instances. Pruitt et al. (2013) develop a non-convex MINLP to describe the design and dispatch of a combined heat and power system using solid oxide fuel cells for commercial buildings over a time horizon of one year.

MIPs that employ linearization and outer-approximation techniques to bound and solve the nonlinear problem can serve as tractable alternatives to MINLPs and yield solutions that approximate realistic dispatch. DER-CAM is a software package developed by Lawrence Berkeley National Laboratory (see, e.g., Stadler et al. 2014) to guide microgrid design with both AC and DC power flow for a set of technologies such as heat pumps, wind power, PV, energy storage, and diesel generators. DER-CAM further includes the option to connect to the grid with associated electricity market considerations. Scioletti et al. (2017) develop a model with a subset of these technologies and DC-only power flow, but track the technologies with finer detail: (i) in terms of an individual component's use by measuring, and accounting for, lifecycles; (ii) through measurements of state-of-charge and power flow through the battery; and, (iii) via fuel curves for diesel generators, which are treated as individual elements that can run isochronous to one another. While the model of DER-CAM is more widely applicable, the model of Scioletti et al. has higher fidelity for key aspects of its motivating application, a military forward operating base.

Our first contribution lies in reducing the error associated with linearizing nonlinear battery power and lifecycle degradation constraints by replacing a single convex envelope with multiple sub-envelopes, which bound the feasible region of the approximation variable for the bilinear term and its components. This also allows for construction of a MINLP-feasible solution to form a high-quality upper bound. Our second contribution is an algorithm that decomposes the time horizon into smaller time periods, which yield subproblems that we solve in parallel to obtain upper and lower bounds on the model's optimal objective function value. While we illustrate the method using the microgrid design and dispatch problem from Scioletti et al. (2017), the approach extends to models that have a strategic decision that impacts operational decisions over a long time horizon, including airlift scheduling (Baker et al. 2002) and capital budgeting (Brown et al. 2004).

The remainder of this paper is organized as follows. Section 2 describes the general model. Section 3 explains the outer-approximation of bilinear terms associated with the

product of battery state-of-charge and current. Section 4 details the decomposition method used to obtain upper and lower bounds on the model's optimal value. Section 5 assesses the performance of the proposed outer-approximation and decomposition algorithm using a collection of instances from the literature. Section 6 concludes and presents possible extensions of this work.

2. Model Description

Our microgrid design and dispatch problem possesses the following properties: (i) the goal is to minimize the cost associated with both a time-invariant strategic decision and a series of time-varying operational (dispatch) decisions; (ii) some operational decisions include relationships modeled with bilinear terms; (iii) the model is loosely coupled with respect to time in that only a few constraints link consecutive time periods via inventory; and, (iv) after specified time intervals, the inventory (state-of-charge) variables must "reset" to the same value. In what follows, we use $t \in \mathcal{T}$ to index time periods, and the system must reset the inventory variables every v time periods, where we assume $|\mathcal{T}|/v$ is an integer.

2.1. ($\mathcal{P}$) Formulation

We formulate our microgrid design and dispatch model using constructs that highlight temporal dependencies and yet are relatively general. This simplifies the notation in our subsequent descriptions of both the linearization schemes for bilinear terms and the decomposition methods with accompanying bounds.

Sets

$t \in \mathcal{T} = \{1, 2, \ldots, \lvert\mathcal{T}\rvert\}$	time periods
$\ell \in \mathcal{L} = \{1, 2, \ldots, \lvert\mathcal{L}\rvert\}$	time blocks indexing a partition of $\mathcal{T}$; i.e., $\cup_{\ell \in \mathcal{L}} \mathcal{T}_\ell = \mathcal{T}$ and $\mathcal{T}_\ell \cap \mathcal{T}_{\ell'} = \emptyset$, $\ell \neq \ell'$
$\mathcal{T}_\ell \subset \mathcal{T}$	time periods in block ℓ
$X \in \mathcal{X}$	strategic design decisions
$Y_t \in \mathcal{Y}_t(X)$	operational decisions made in time period t, given decision X

Functions

$f_0(\cdot)$	cost of a design decision
$f_t(\cdot)$	cost of an operational decision at time period t

$g_t(\cdot)$	net change in inventory associated with an operational decision at time period t

Parameters

υ	number of time periods per block

With these constructs, we have:

$$\mathcal{T}_\ell = \{(\ell-1)\upsilon+1, (\ell-1)\upsilon+2, \ldots, \ell\upsilon\},\ \forall \ell \in \mathcal{L}.$$

Decision Variables

X	strategic design decision
R	strategic inventory reset value
Y_t	operational decision at time period t; $Y = (Y_t)_{t\in\mathcal{T}}$
$\underline{Y}_t$	inventory at start of time period t; $\underline{Y} = (\underline{Y}_t)_{t\in\mathcal{T}}$
$\bar{Y}_t$	inventory at end of time period t; $\bar{Y} = (\bar{Y}_t)_{t\in\mathcal{T}}$

Boundary Condition

Y_0	initial inventory

($\mathcal{P}$) Formulation

$$z^P = \min_{X,R,Y,\underline{Y},\bar{Y}} f_0(X) + \sum_{t\in\mathcal{T}} f_t(Y_t) \tag{1a}$$

$$\text{s.t.} \quad X \in \mathcal{X} \tag{1b}$$

$$Y_t \in \mathcal{Y}_t(X), \quad \forall t \in \mathcal{T} \tag{1c}$$

$$\bar{Y}_t = \underline{Y}_t + g_t(Y_t), \quad \forall t \in \mathcal{T} \tag{1d}$$

$$\underline{Y}_t = \bar{Y}_{t-1}, \quad \forall t \in \mathcal{T}\setminus\{1\} \tag{1e}$$

$$\underline{Y}_{(\ell-1)\cdot\upsilon+1} = R, \quad \forall \ell \in \mathcal{L}\setminus\{1\} \tag{1f}$$

$$\underline{Y}_1 = Y_0 \tag{1g}$$

Through the objective in (1a), we seek a minimum-cost set of strategic and operational decisions. This objective includes the cost of battery degradation, which grows with deeper

levels of discharge; therefore, we model lifecycles spent as a function of battery current and state-of-charge, which involves the product of the two. Constraint (1b) specifies feasible strategic designs, as defined by the set $\mathcal{X}$. Constraint (1c) restricts operational decisions Y_t to those allowable by the design decision X at each time period t; for example, only an asset purchased as part of a design decision may be operated at time period t. More generally, constraint (1c) includes nonlinear relationships, which we detail in Section 2.2. Constraint (1d) captures changes in inventory from the start to the end of a given time period. Constraint (1e) reconciles the inventory between the end of one time period and the beginning of the next. Constraint (1f) enforces our reset policy by restricting the inventory at the boundaries of the time blocks to be the same. The reset policy limits the number of future time periods the model may use to inform dispatch decisions, and hence limits the model's ability to over-optimize dispatch to future variations in load. Constraint (1g) fixes the starting inventory to the boundary condition. The strategic decisions X and R, along with inventory constraints (1e), couple decisions across time. In Section 4, we develop a method that decomposes model (1) into $|\mathcal{L}|$ subproblems, in which the respective subproblems correspond to decisions within blocks $\mathcal{T}_\ell$, $\ell \in \mathcal{L}$.

2.2. ($\mathcal{M}$) Formulation: Linearization of ($\mathcal{P}$)

A subset of the relationships within constraint (1c), such as battery lifecycles spent as a function of current and state-of-charge, include bilinear terms. We can linearize these bilinear terms using ideas that begin with McCormick (1976) and include significant subsequent work such as Androulakis et al. (1995). Let Y_{1t} and Y_{2t} denote two components of operational decision Y_t that contribute a nonlinear term to constraint (1c), and let auxiliary decision variable Z_t represent the product $Y_{1t} \cdot Y_{2t}$. McCormick (1976) presents an outer-approximation that replaces the bilinear relationship

$$Z_t = Y_{1t} \cdot Y_{2t}, \quad \forall t \in \mathcal{T}, \tag{2}$$

with a convex envelope to constrain Z_t, allowing for the reformulation of ($\mathcal{P}$) as an approximating MIP, i.e., as a linear mixed-integer program. The outer-approximation used in McCormick (1976) is as follows:

Additional Decision Variables

Y_{1t}, Y_{2t}	two components of operational decision vector Y_t that form a bilinear relationship
Z_t	linear approximation variable representing the product $Y_{1t} \cdot Y_{2t}$

Additional Parameters

u_1	upper bound of operational component variable Y_{1t}
l_1	lower bound of operational component variable Y_{1t}
u_2	upper bound of operational component variable Y_{2t}
l_2	lower bound of operational component variable Y_{2t}

Formulation

$$Z_t \geq u_2 Y_{1t} + u_1 Y_{2t} - u_1 u_2, \quad \forall t \in \mathcal{T} \tag{3a}$$

$$Z_t \geq l_2 Y_{1t} + l_1 Y_{2t} - l_1 l_2, \quad \forall t \in \mathcal{T} \tag{3b}$$

$$Z_t \leq l_2 Y_{1t} + u_1 Y_{2t} - u_1 l_2, \quad \forall t \in \mathcal{T} \tag{3c}$$

$$Z_t \leq u_2 Y_{1t} + l_1 Y_{2t} - l_1 u_2, \quad \forall t \in \mathcal{T} \tag{3d}$$

Our application has time-invariant lower and upper bounds (l_1, u_1) and (l_2, u_2) for Y_{1t} and Y_{2t}, respectively, though this assumption may be relaxed in general. We refer to the formulation that starts with $(\mathcal{P})$ and replaces equation (2), which is a part of constraint (1c), with the relaxation described in constraints (3a)-(3d) as model $(\mathcal{M})$, or the *McCormick relaxation*.

2.3. Application to Microgrid Design and Dispatch Problem

Model $(\mathcal{M})$ specializes to the microgrid design and dispatch problem by mapping the strategic design vector X to the number and type of diesel generators, PV systems, and batteries in the design, and by mapping the operational decision vector Y_t to power input and output for each asset, and fuel consumption for each time period. Decision vectors $\underline{Y}$ and $\bar{Y}$ denote the available battery storage at the start and end of each time period, respectively. The variable R denotes the available battery storage at the beginning and end of each specified time block; this reset value is identical across all time blocks to simplify the dispatch policy and to limit appropriate adaptation of the dispatch policy to future

load. In some applications, this target may be a prespecified level of inventory; however, in what follows, we optimize this value. Because the load and PV availability exhibit diurnal patterns, we select the duration of a time block to be a day.

Our application assumes that a diesel generator consumes a fixed amount of fuel per time period when running, in addition to a variable amount that is a linear function of the power output. Therefore, to maximize efficiency, it is preferable to run a diesel generator at its rated capacity. However, in response to rapid changes in load, one generator may run isochronous to the others. For this reason, in the MINLP in Scioletti et al. (2017), multiple copies of the same generators are modeled as "twins," each of which has an independent decision variable for power output at each time period. While the general problem may include twins of the same battery technology, the instances in Scioletti et al. (2017) restrict the solution to include at most one battery; this assumption is tantamount to honoring the policy in which batteries operate in droop, rather than individually, to avoid a situation in which one battery is used to charge another. This high-level mapping suffices for our immediate purposes; however, the full microgrid design and dispatch model is detailed in the Online Supplement, largely following the model of Scioletti et al. (2017).

3. Reducing Linearization Error in $(\mathcal{M})$

The envelope described in constraints (3a)-(3d) represents the tightest possible convex relaxation for a bilinear term (Al-Khayyal and Falk 1983); however, the relaxation in these models may neither yield sufficiently tight lower bounds on $(\mathcal{P})$'s optimal value, nor produce implementable solutions to the nonlinear model. Further, constructing a feasible solution to $(\mathcal{P})$ by starting with a solution to $(\mathcal{M})$ may provide a low-quality upper bound on $(\mathcal{P})$. Bergamini et al. (2005) and Karuppiah and Grossman (2006) tighten this relaxation by subdividing the interval defined by the simple bounds of each component; we refer to this technique as *partitioning*. We introduce binary variables that determine which subregion defines the active constraints for Y_{1t}, Y_{2t}, and Z_t for each time period, and we refer to these as *subregion activation variables*. Figure 1 shows an example of such a subdivision when partitioning the domain of Y_{2t}. Both Wicaksono and Karimi (2008) and Gounaris et al. (2009) derive ways to partition McCormick's relaxation, noting that the computational performance of these formulations is impossible to predict; however, Gounaris et al. (2009) identify ten partitioning schemes that computationally outperform the other methods they present.

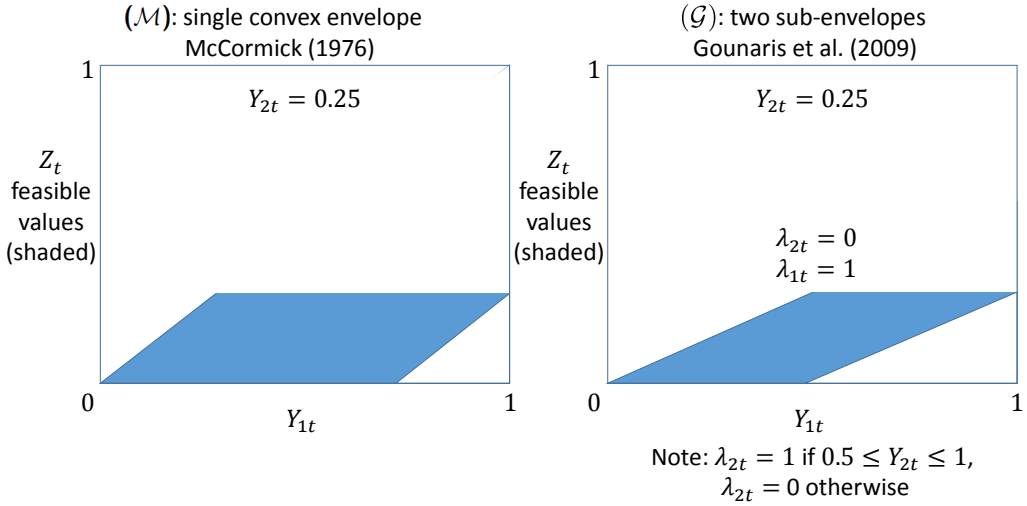

Figure 1: Example of subdividing the McCormick envelope given $Y_{2t} = 0.25$, shown on the left-hand side, by partitioning on one variable, in which we linearize $Y_{1t} \cdot Y_{2t}$. In this example, Y_{1t} and Y_{2t} have simple bounds $l_1 = l_2 = 0$ and $u_1 = u_2 = 1$. The shape on the right-hand side represents the sub-envelope that defines the feasible region for Y_{1t} and Z_t, with binary subregion activation variables; see subsequent constraints (8) and associated variables.

At a computational cost, partitioning reduces the approximation error, which can improve lower bounds on, and allow for the construction of, a higher-quality solution to model ($\mathcal{P}$) when using the resulting linear MIP solution as a starting point. Partitioning requires binary restrictions to activate sub-envelopes, and introduces additional variables and constraints that grow linearly with the number of total subregions, both of which may compromise tractability. Vielma et al. (2010a) and Vielma and Nemhauser (2010b) present a model for piecewise-linear functions in which the number of binary variables scales logarithmically with the number of segments; Misener et al. (2011) use this model to implement a partitioning scheme that they then apply to the pooling problem, and show that the linear partitioning technique we adopt is preferable for situations in which the number of partitions is relatively low (eight or fewer subregions in their work).

If one component in the bilinear term can be discretized to a finite number of reference values in place of a continuous domain, an exact linearization can be performed; see, e.g., Dvorkin et al. (2017). Similarly, Gupte et al. (2013) provide an exact reformulation for the product of a nonnegative integer variable and a nonnegative continuous variable. The former is replaced by its binary expansion, and a McCormick envelope linearizes the resulting product. The authors develop the convex hull of the corresponding MIP set.

Castro (2015) presents a univariate partitioning scheme that specifies lower and upper bounds on both components of the bilinear term for each subregion, and applies the procedure to a subset of the cases in Gounaris et al. (2009). In Section 3.1, we reformulate a different case from Gounaris et al. (2009) that reduces to a single McCormick envelope when binary restrictions on the subregion activation variables are relaxed; our improvement applies to both univariate and bivariate partitioning schemes.

3.1. Partitioning Approach

For a given relaxation of $Z_t = Y_{1t} \cdot Y_{2t}$, we define the *approximation error* as a function of Y_{1t} as:

$$\mathcal{E}(Y_{1t}) = \max_{Y_{2t}, Z_t} [Z_t - Y_{1t} \cdot Y_{2t}], \tag{4}$$

in which the maximization over Y_{2t} and Z_t is constrained by the simple bounds on Y_{2t}, and the appropriate subregion depending on the outer-approximation in use, e.g., constraints (3a)-(3d) if model ($\mathcal{M}$) is used. For the McCormick relaxation, $\mathcal{E}(Y_{1t})$ is maximized at the midpoint of the interval $[l_1, u_1]$, and this maximized value is one fourth of the area defined by the simple bounds on Y_{1t} and Y_{2t}, i.e., $(u_1 - l_1) \cdot (u_2 - l_2)/4$ (Androulakis et al. 1995).

Applying a partitioning scheme to the McCormick relaxation by creating m uniform subregions on the domain of one variable in the bilinear term (Bergamini et al. 2005, Karuppiah and Grossman 2006) decreases the worst-case approximation error by a factor of m to:

$$\frac{1}{m} \quad \frac{(u_1 - l_1)(u_2 - l_2)}{4} \Bigg) . \Bigg($$

Hasan and Karimi (2010) present a bivariate partitioning scheme, which creates m uniform subregions on one variable and n uniform subregions on the other in the bilinear term. In this setting, the worst-case approximation error decreases by a factor of mn, to:

$$\frac{1}{mn} \quad \frac{(u_1 - l_1)(u_2 - l_2)}{4} \Bigg) . \Bigg($$

Figure 2 depicts the maximum approximation error, $\mathcal{E}(Y_{1t})$, as a function of Y_{1t} when partitioning on one or both variables. Nonuniform partitions, such as those described in Wicaksono and Karimi (2008), are possible, and even advisable, if partitioning is done dynamically in the course of solving the problem; Nagarajan et al. (2016) demonstrate

the effectiveness of such an approach in solving large-scale MINLPs. However, we focus on uniform partitions built a priori, which minimize the worst-case approximation error (Hasan and Karimi 2010). Dey and Gupte (2015) provide solution quality guarantees for applications of partitioning schemes to pooling problems, and show empirically that, for their application, a uniform partitioning scheme outperforms an asymmetric approach.

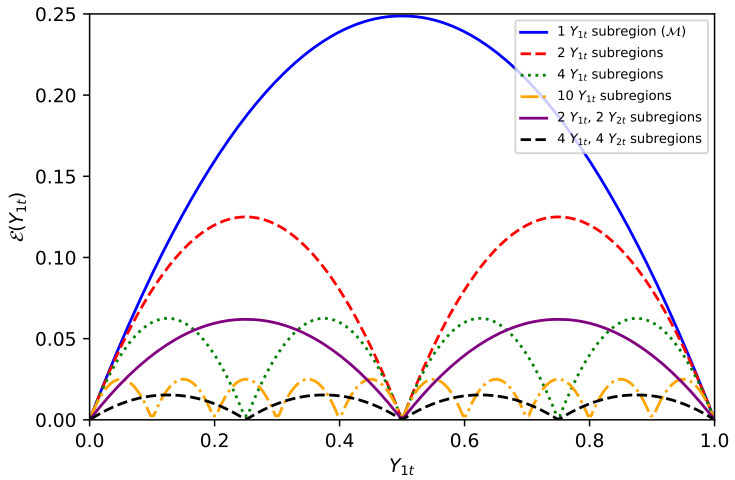

Figure 2: Approximation error per equation (4), as a function of Y_{1t} under partitioning schemes for different numbers of uniform subregions, using partitioning on Y_{1t} only, and on both Y_{1t} and Y_{2t}, respectively. This figure assumes that the range of both Y_{1t} and Y_{2t} is [0,1].

Section 3.2 presents the constraints we propose by partitioning on the variables Y_{1t} and Y_{2t}. We replace the McCormick relaxation in ($\mathcal{M}$) with new constraints from this approach to approximate the bilinear terms in ($\mathcal{P}$), and we refer to the resulting model as ($\mathcal{U}$) because it underestimates ($\mathcal{P}$).

3.2. ($\mathcal{U}$) Formulation

Our scheme partitions the feasible region into subregions according to intervals in the domain of Y_{1t}, which we index by $m \in \mathcal{M}$. So, we augment the simple bounds of u_1 and l_1 with boundaries for each active subregion u_{1m} and l_{1m}, $\forall m \in \mathcal{M}$, in which $l_{1,1} = l_1$, $u_{1,|\mathcal{M}|} = u_1$, and $l_{1,m} = u_{1,m-1}$, $\forall m \in \mathcal{M} \setminus \{1\}$; we perform an analogous augmentation of the simple bounds of u_2 and l_2, which we index by $n \in \mathcal{N}$.

We introduce binary subregion activation variables to indicate which constraints define the active part of the feasible region for Y_{1t}, Y_{2t}, and Z_t when assigned a value of one; the constraints relax to nominal McCormick bounds otherwise.

Additional Sets

$m \in \mathcal{M} = \{1, 2, \ldots, \lvert\mathcal{M}\rvert\}$	set of subregions obtained by partitioning the domain of Y_{1t}
$n \in \mathcal{N} = \{1, 2, \ldots, \lvert\mathcal{N}\rvert\}$	set of subregions obtained by partitioning the domain of Y_{2t}

Additional Parameters

l_{1m}	lower bound for Y_{1t} within subregion m
u_{1m}	upper bound for Y_{1t} within subregion m
l_{2n}	lower bound for Y_{2t} within subregion n
u_{2n}	upper bound for Y_{2t} within subregion n

Additional Decision Variables

λ_{mnt}	1 if subregion (m, n) defines the active part of the feasible region of Y_{1t}, Y_{2t}, and Z_t in period t, 0 otherwise [binary]

Formulation

The following set of constraints represents partitioning on both Y_{1t} and Y_{2t}, which we tailor from formulation `NF2g`, the fastest-performing partitioning scheme of those described in Gounaris et al. (2009) when implemented for our application. Scioletti (2016a) details the performance of alternative partitioning schemes from Gounaris et al. when applied to the microgrid design and dispatch problem.

$$\sum_{m \in \mathcal{M}} \sum_{n \in \mathcal{N}} \lambda_{mnt} = 1, \quad \forall t \in \mathcal{T} \tag{5a}$$

$$Y_{1t} \geq l_1 + (l_{1m} - l_1)\lambda_{mnt}, \quad \forall m \in \mathcal{M}, n \in \mathcal{N}, t \in \mathcal{T} \tag{5b}$$

$$Y_{1t} \leq u_1 - (u_1 - u_{1m})\lambda_{mnt}, \quad \forall m \in \mathcal{M}, n \in \mathcal{N}, t \in \mathcal{T} \tag{5c}$$

$$Y_{2t} \geq l_2 + (l_{2n} - l_2)\lambda_{mnt}, \quad \forall m \in \mathcal{M}, n \in \mathcal{N}, t \in \mathcal{T} \tag{5d}$$

$$Y_{2t} \leq u_2 - (u_2 - u_{2n})\lambda_{mnt}, \quad \forall m \in \mathcal{M}, n \in \mathcal{N}, t \in \mathcal{T} \tag{5e}$$

$$Z_t \geq u_{2n}Y_{1t} + u_{1m}Y_{2t} - u_{1m}u_{2n} - (u_1u_2 - u_{1m}u_{2n} - (u_2 - u_{2n})l_1 - (u_1 - u_{1m})l_2)(1 - \lambda_{mnt}), \quad \forall m \in \mathcal{M}, n \in \mathcal{N}, t \in \mathcal{T} \tag{5f}$$

$$Z_t \geq l_{2n}Y_{1t} + l_{1m}Y_{2t} - l_{1m}l_{2n} - (l_1l_2 - l_{1m}l_{2n} - (l_2 - l_{2n})u_1 - (l_1 - l_{1m})u_2)(1 - \lambda_{mnt}), \quad \forall m \in \mathcal{M}, n \in \mathcal{N}, t \in \mathcal{T} \tag{5g}$$

$$Z_t \leq l_{2n}Y_{1t} + u_{1m}Y_{2t} - u_{1m}l_{2n} + (u_{1m}l_{2n} - u_1l_2 + (l_2 - l_{2n})l_1 + (u_1 - u_{1m})u_2)(1 - \lambda_{mnt}),$$

$$\forall m \in \mathcal{M}, n \in \mathcal{N}, t \in \mathcal{T} \tag{5h}$$

$$Z_t \leq u_{2n}Y_{1t} + l_{1m}Y_{2t} - l_{1m}u_{2n} + (l_{1m}u_{2n} - l_1u_2 + (u_2 - u_{2n})u_1 + (l_1 - l_{1m})l_2)(1 - \lambda_{mnt}),$$

$$\forall m \in \mathcal{M}, n \in \mathcal{N}, t \in \mathcal{T} \tag{5i}$$

$$\lambda_{mnt} \in \{0, 1\}, \quad \forall m \in \mathcal{M}, n \in \mathcal{N}, t \in \mathcal{T} \tag{5j}$$

Constraint (5a) requires exactly one of the subregion activation variables λ_{mnt} to assume a value of one for each time period t. Constraints (5b)-(5e) restrict Y_{1t} and Y_{2t} to each variable's active subregion. If λ_{mnt}=1, then subregion (m, n) is active, and Y_{1t} and Y_{2t} are restricted to the intervals $[l_{1m}, u_{1m}]$ and $[l_{2n}, u_{2n}]$, respectively. If λ_{mnt}=0, the constraints reduce to simple bounds on Y_{1t} and Y_{2t}.

The McCormick relaxation uses four constraints to restrict Z_t as a function of the components Y_{1t} and Y_{2t} and their simple bounds. The partitioning scheme reduces the size of the active subregion, which allows for a smaller convex envelope, i.e., sub-envelope, which, in turn, yields a tighter relaxation. Constraints (5f) through (5i) bound Z_t according to the sub-envelope chosen by the subregion activation variables, λ_{mnt}. If λ_{mnt}=1, then Z_t is constrained by the convex envelope of the active subregion. If a subregion is not active, the associated constraints are dominated by McCormick bounds.

As we show in Proposition 1, if $\lambda_{mnt} = 1$, then the partitioning scheme of Gounaris et al. (2009) generates constraints (5), except that the last term in their analog of constraints (5f)-(5i) is $(u_1 - l_1)(u_2 - l_2)(1 - \lambda_{mnt})$ whose coefficient is the smallest value that reduces constraints (5f)-(5i) to simple bounds on Y_{1t} and Y_{2t} when $\lambda_{mnt} = 0$. Our approach differs from Gounaris et al. in that we find the smallest such value for each individual constraint, rather than a single value to apply to all constraints. When we use the approach in Gounaris et al. (2009) rather than constraints (5) to approximate the bilinear terms in $(\mathcal{P})$, we call the resulting model $(\mathcal{G})$. Proposition 1 characterizes the relative tightness of formulations $(\mathcal{U})$, $(\mathcal{G})$, and $(\mathcal{M})$. Our formulation is tighter than $(\mathcal{G})$ because when $\lambda_{mnt} = 0$, our constraints (5) revert to McCormick bounds, while the analogous constraints in $(\mathcal{G})$ relax to simple bounds. To streamline the notation, we drop the t index, and treat Y_1, Y_2, and Z as scalar decision variables in the proposition.

PROPOSITION 1. *Let* $m \in \mathcal{M} = \{1,2,\ldots,|\mathcal{M}|\}$, *and* l_{1m}, u_{1m} *satisfy* $l_{1,1} = l_1$, $u_{1,|\mathcal{M}|} = u_1$, *and* $l_{1m} = u_{1,m-1}$, $l_{1,m-1} < l_{1m}$, $u_{1,m-1} < u_{1m}$, $\forall m \in \mathcal{M} \setminus \{1\}$. *Likewise, let* $n \in \mathcal{N} = \{1,2,\ldots,|\mathcal{N}|\}$, *and* l_{2n}, u_{2n} *satisfy* $l_{2,1} = l_2$, $u_{2,|\mathcal{N}|} = u_2$, *and* $l_{2,n} = u_{2,n-1}$, $l_{2,n-1} < l_{2n}$, $u_{2,n-1} < u_{2n}$, $\forall n \in \mathcal{N} \setminus \{1\}$. *Let*

$$S = \{(Y_1, Y_2, Z) : Z = Y_1 \cdot Y_2,\ l_1 \le Y_1 \le u_1,\ l_2 \le Y_2 \le u_2\},$$

and

$$\begin{aligned} S^M = \{(Y_1, Y_2, Z) :\ & Z \ge u_2 Y_1 + u_1 Y_2 - u_1 u_2, \\ & Z \ge l_2 Y_1 + l_1 Y_2 - l_1 l_2, \\ & Z \le l_2 Y_1 + u_1 Y_2 - u_1 l_2, \\ & Z \le u_2 Y_1 + l_1 Y_2 - l_1 u_2, \\ & l_1 \le Y_1 \le u_1,\ l_2 \le Y_2 \le u_2\}. \end{aligned}$$

Define

$$Y_1 \ge l_1 + (l_{1m} - l_1)\lambda_{mn},\ \forall m \in \mathcal{M}, n \in \mathcal{N} \tag{6a}$$

$$Y_1 \le u_1 - (u_1 - u_{1m})\lambda_{mn},\ \forall m \in \mathcal{M}, n \in \mathcal{N} \tag{6b}$$

$$Y_2 \ge l_2 + (l_{2n} - l_2)\lambda_{mn},\ \forall m \in \mathcal{M}, n \in \mathcal{N} \tag{6c}$$

$$Y_2 \le u_2 - (u_2 - u_{2n})\lambda_{mn},\ \forall m \in \mathcal{M}, n \in \mathcal{N} \tag{6d}$$

$$Z \ge u_{2n} Y_1 + u_{1m} Y_2 - u_{1m} u_{2n} - a_{mn}(1 - \lambda_{mn}),\ \forall m \in \mathcal{M}, \forall n \in \mathcal{N} \tag{6e}$$

$$Z \ge l_{2n} Y_1 + l_{1m} Y_2 - l_{1m} l_{2n} - b_{mn}(1 - \lambda_{mn}),\ \forall m \in \mathcal{M}, \forall n \in \mathcal{N} \tag{6f}$$

$$Z \le l_{2n} Y_1 + u_{1m} Y_2 - u_{1m} l_{2n} + c_{mn}(1 - \lambda_{mn}),\ \forall m \in \mathcal{M}, \forall n \in \mathcal{N} \tag{6g}$$

$$Z \le u_{2n} Y_1 + l_{1m} Y_2 - l_{1m} u_{2n} + d_{mn}(1 - \lambda_{mn}),\ \forall m \in \mathcal{M}, \forall n \in \mathcal{N}. \tag{6h}$$

Let

$$\begin{aligned} S^G = \{(Y_1, Y_2, Z) : (6)\ \textit{with}\ & a_{mn} = b_{mn} = c_{mn} = d_{mn} = (u_1 - l_1)(u_2 - l_2), \\ & l_1 \le Y_1 \le u_1,\ l_2 \le Y_2 \le u_2, \\ & \sum_{m \in \mathcal{M}} \sum_{n \in \mathcal{N}} \lambda_{mn} = 1,\ \lambda_{mn} \in \{0,1\},\ \forall m \in \mathcal{M}, n \in \mathcal{N}\} \end{aligned}$$

and

$$\begin{aligned} S^U = \{(Y_1, Y_2, Z) : (6) \text{ with } a_{mn} &= u_1u_2 - u_{1m}u_{2n} - (u_2 - u_{2n})l_1 - (u_1 - u_{1m})l_2, \\ b_{mn} &= l_1l_2 - l_{1m}l_{2n} - (l_2 - l_{2n})u_1 - (l_1 - l_{1m})u_2, \\ c_{mn} &= u_{1m}l_{2n} - u_1l_2 + (l_2 - l_{2n})l_1 + (u_1 - u_{1m})u_2, \\ d_{mn} &= l_{1m}u_{2n} - l_1u_2 + (u_2 - u_{2n})u_1 + (l_1 - l_{1m})l_2, \\ l_1 \le Y_1 \le u_1,\ & l_2 \le Y_2 \le u_2, \\ \sum_{m\in\mathcal{M}}\sum_{n\in\mathcal{N}} \lambda_{mn} = 1,\ & \lambda_{mn} \in \{0,1\},\ \forall m \in \mathcal{M}, n \in \mathcal{N}\}. \end{aligned}$$

Then, $S \subseteq S^U \subseteq S^G \subseteq S^M = S^U_{LP} \subseteq S^G_{LP}$, where S^U_{LP} and S^G_{LP} represent the linear programming relaxation of S^U and S^G, respectively; i.e., with $\lambda_{mn} \in \{0,1\}$ replaced by $0 \le \lambda_{mn} \le 1$, $\forall m \in \mathcal{M}, n \in \mathcal{N}$. Moreover, $S \subseteq S^U$, $S^G \subseteq S^M$, and $S^U_{LP} \subseteq S^G_{LP}$ can be strict.

Proof. First, we let $(Y_1, Y_2, Z) \in S$, and show $(Y_1, Y_2, Z) \in S^U$. To this end, let $\lambda_{\bar{m}\bar{n}} = 1$ for an interval satisfying $Y_1 \in [l_{1\bar{m}}, u_{1\bar{m}}]$ and $Y_2 \in [l_{2\bar{n}}, u_{2\bar{n}}]$, breaking ties arbitrarily, and let $\lambda_{mn} = 0,\ \forall m \in \mathcal{M}, n \in \mathcal{N} : (m,n) \ne (\bar{m},\bar{n})$. For $(m,n) \ne (\bar{m},\bar{n})$, constraints (6a)-(6d) yield $l_1 \le Y_1 \le u_1$, $l_2 \le Y_2 \le u_2$, and for $(m,n) = (\bar{m},\bar{n})$, these constraints yield $l_{1m} \le Y_1 \le u_{1m}$, $l_{2n} \le Y_2 \le u_{2n}$. Consider constraints (6e)-(6h). For $(m,n) = (\bar{m},\bar{n})$, these constraints yield

$$Z \ge u_{2n}Y_1 + u_{1m}Y_2 - u_{1m}u_{2n} \tag{7a}$$

$$Z \ge l_{2n}Y_1 + l_{1m}Y_2 - l_{1m}l_{2n} \tag{7b}$$

$$Z \le l_{2n}Y_1 + u_{1m}Y_2 - u_{1m}l_{2n} \tag{7c}$$

$$Z \le u_{2n}Y_1 + l_{1m}Y_2 - l_{1m}u_{2n}. \tag{7d}$$

The following shows that constraint (7a) holds for $(Y_1, Y_2, Z) \in S$ with $Y_1 \in [l_{1\bar{m}}, u_{1\bar{m}}]$ and $Y_2 \in [l_{2\bar{n}}, u_{2\bar{n}}]$:

$$\begin{aligned} 0 &\le (u_{1m} - Y_1)(u_{2n} - Y_2) \\ 0 &\le Y_1Y_2 - u_{2n}Y_1 - u_{1m}Y_2 + u_{1m}u_{2n} \\ Z &\ge u_{2n}Y_1 + u_{1m}Y_2 - u_{1m}u_{2n}. \end{aligned}$$

Similarly, constraints (7b)-(7d) hold via:

$$\begin{aligned} 0 \le (Y_1 - l_{1m})(Y_2 - l_{2n}) &\Rightarrow Z \ge l_{2n}Y_1 + l_{1m}Y_2 - l_{1m}l_{2n} \\ 0 \le (u_{1m} - Y_1)(Y_2 - l_{2n}) &\Rightarrow Z \le l_{2n}Y_1 + u_{1m}Y_2 - u_{1m}l_{2n} \\ 0 \le (Y_1 - l_{1m})(u_{2n} - Y_2) &\Rightarrow Z \le u_{2n}Y_1 + l_{1m}Y_2 - l_{1m}u_{2n}. \end{aligned}$$

Therefore, (Y_1, Y_2, Z) satisfies constraints (6e)-(6h) for $(m,n) = (\bar{m}, \bar{n})$. If $(m,n) \neq (\bar{m}, \bar{n})$, the right-hand sides of these constraints for S^U are dominated by those of the McCormick relaxation of S^M; i.e.,

$$\begin{aligned}
\text{(6e)}: \quad & u_{2n}Y_1 + u_{1m}Y_2 - u_{1m}u_{2n} - (u_1u_2 - u_{1m}u_{2n} - (u_2 - u_{2n})l_1 - (u_1 - u_{1m})l_2) \\
& = u_{2n}Y_1 + u_{1m}Y_2 - u_1u_2 + (u_2 - u_{2n})l_1 + (u_1 - u_{1m})l_2 \\
& \leq u_{2n}Y_1 + u_{1m}Y_2 - u_1u_2 + (u_2 - u_{2n})Y_1 + (u_1 - u_{1m})Y_2 \\
& = u_2Y_1 + u_1Y_2 - u_1u_2 \quad \forall (m,n) \in \mathcal{M} \times \mathcal{N} \setminus \{(\bar{m}, \bar{n})\} \\
\text{(6f)}: \quad & l_{2n}Y_1 + l_{1m}Y_2 - l_{1m}l_{2n} - (l_1l_2 - l_{1m}l_{2n} - (l_2 - l_{2n})u_1 - (l_1 - l_{1m})u_2) \\
& = l_{2n}Y_1 + l_{1m}Y_2 - l_1l_2 - (l_{2n} - l_2)u_1 - (l_{1m} - l_1)u_2 \\
& \leq l_{2n}Y_1 + l_{1m}Y_2 - l_1l_2 - (l_{2n} - l_2)Y_1 - (l_{1m} - l_1)Y_2 \\
& = l_2Y_1 + l_1Y_2 - l_1l_2 \quad \forall (m,n) \in \mathcal{M} \times \mathcal{N} \setminus \{(\bar{m}, \bar{n})\} \\
\text{(6g)}: \quad & l_{2n}Y_1 + u_{1m}Y_2 - u_{1m}l_{2n} + (u_{1m}l_{2n} - u_1l_2 + (l_2 - l_{2n})l_1 + (u_1 - u_{1m})u_2) \\
& = l_{2n}Y_1 + u_{1m}Y_2 - u_1l_2 + (l_2 - l_{2n})l_1 + (u_1 - u_{1m})u_2 \\
& \geq l_{2n}Y_1 + u_{1m}Y_2 - u_1l_2 + (l_2 - l_{2n})Y_1 + (u_1 - u_{1m})Y_2 \\
& = l_2Y_1 + u_1Y_2 - u_1l_2 \quad \forall (m,n) \in \mathcal{M} \times \mathcal{N} \setminus \{(\bar{m}, \bar{n})\} \\
\text{(6h)}: \quad & u_{2n}Y_1 + l_{1m}Y_2 - l_{1m}u_{2n} + (l_{1m}u_{2n} - l_1u_2 + (u_2 - u_{2n})u_1 + (l_1 - l_{1m})l_2) \\
& = u_{2n}Y_1 + l_{1m}Y_2 - l_1u_2 + (u_2 - u_{2n})u_1 + (l_1 - l_{1m})l_2 \\
& \geq u_{2n}Y_1 + l_{1m}Y_2 - l_1u_2 + (u_2 - u_{2n})Y_1 + (l_1 - l_{1m})Y_2 \\
& = u_2Y_1 + l_1Y_2 - l_1u_2 \quad \forall (m,n) \in \mathcal{M} \times \mathcal{N} \setminus \{(\bar{m}, \bar{n})\}.
\end{aligned}$$

Therefore, (Y_1, Y_2, Z) satisfies constraints (6e)-(6h) when $(m,n) \neq (\bar{m}, \bar{n})$, and so $(Y_1, Y_2, Z) \in S \Rightarrow (Y_1, Y_2, Z) \in S^U$.

Suppose $(Y_1, Y_2, Z) \in S^U$. The constraints of S^G are identical to those of S^U for $(m,n) = (\bar{m}, \bar{n})$, and S^U has tighter constraints than S^G when $(m,n) \neq (\bar{m}, \bar{n})$, because the values for a_{mn}, b_{mn}, c_{mn}, and d_{mn} in S^U are smaller than the analogous terms specified in the definition of S^G; i.e.,

$$\begin{aligned}
\text{(6e)}: \quad & (u_1 - l_1)(u_2 - l_2) - (u_1u_2 - u_{1m}u_{2n} - (u_2 - u_{2n})l_1 - (u_1 - u_{1m})l_2) \\
& = (u_{1m} - l_1)(u_{2n} - l_2) \geq 0
\end{aligned}$$

$$
\begin{aligned}
\text{(6f)}: \quad & (u_1 - l_1)(u_2 - l_2) - (l_1 l_2 - l_{1m} l_{2n} - (l_2 - l_{2n})u_1 - (l_1 - l_{1m})u_2) \\
& = (u_1 - l_{1m})(u_2 - l_{2n}) \geq 0 \\
\text{(6g)}: \quad & (u_1 - l_1)(u_2 - l_2) - (u_{1m} l_{2n} - u_1 l_2 + (l_2 - l_{2n})l_1 + (u_1 - u_{1m})u_2) \\
& = (u_{1m} - l_1)(u_2 - l_{2n}) \geq 0 \\
\text{(6h)}: \quad & (u_1 - l_1)(u_2 - l_2) - (l_{1m} u_{2n} - l_1 u_2 + (u_2 - u_{2n})u_1 + (l_1 - l_{1m})l_2) \\
& = (u_1 - l_{1m})(u_{2n} - l_2) \geq 0.
\end{aligned}
$$

Therefore, $(Y_1, Y_2, Z) \in S^U \Rightarrow (Y_1, Y_2, Z) \in S^G$ and $(Y_1, Y_2, Z) \in S^U_{LP} \Rightarrow (Y_1, Y_2, Z) \in S^G_{LP}$.

Suppose $(Y_1, Y_2, Z) \in S^G$, $Y_1 \in [l_{1\bar{m}}, u_{1\bar{m}}]$, and $Y_2 \in [l_{2\bar{n}}, u_{2\bar{n}}]$. We restrict our attention to the constraints for $(m, n) = (\bar{m}, \bar{n})$, which dominate those for $(m, n) \neq (\bar{m}, \bar{n})$. Using a similar argument to that for $S \subseteq S^U$ above, we can show that the first constraint of S^M holds:

$$
\begin{aligned}
& 0 \leq (u_{1m} - Y_1)(u_{2n} - Y_2) \\
& 0 \leq Y_1 Y_2 - u_{1m} Y_2 + u_{2n}(u_{1m} - Y_1) \leq Y_1 Y_2 - u_{1m} Y_2 + u_2(u_{1m} - Y_1) \\
& 0 \leq Y_1 Y_2 - u_2 Y_1 + u_{1m}(u_2 - Y_2) \leq Y_1 Y_2 - u_2 Y_1 + u_1(u_2 - Y_2) \\
& Z \geq u_2 Y_1 + u_1 Y_2 - u_1 u_2.
\end{aligned}
$$

Analogous arguments show that the next three constraints of S^M also hold; hence, $(Y_1, Y_2, Z) \in S^G \Rightarrow (Y_1, Y_2, Z) \in S^M$.

For $(m, n) = (|\mathcal{M}|, |\mathcal{N}|)$, $u_{1m} = u_1$ and $u_{2n} = u_2$, so $a_{mn} = 0$, and constraint (6e) replicates the first constraint in S^M. Likewise, the pairs $(1, 1), (|\mathcal{M}|, 1)$, and $(1, |\mathcal{N}|)$ yield instances of constraints (6f), (6g), and (6h) that are equivalent to the second, third, and fourth constraints in S^M, respectively. This shows that $S^U_{LP} \subseteq S^M$. However, the extreme points of S^M are:

$$
S^M_e = \{(u_1, u_2, u_1 u_2), (l_1, l_2, l_1 l_2), (u_1, l_2, u_1 l_2), (l_1, u_2, l_1 u_2)\},
$$

all of which are points in S and, by extension, S^U_{LP}. Further, because S^U_{LP} is convex, $\text{conv}(S^M_e) = S^M \subseteq S^U_{LP}$. Therefore, $S^M = S^U_{LP}$.

For examples showing that the relationships $S \subseteq S^U$ and $S^G \subseteq S^M$ can be strict, let $l_1 = l_2 = 0$, $u_1 = u_2 = 1$, $|\mathcal{M}| = 1$, and $|\mathcal{N}| = 2$ with intervals of equal length. Then, $(Y_1, Y_2, Z) = (0.6, 0.6, 0.4) \in S^U$ but $(0.6, 0.6, 0.4) \notin S$, and $(0.6, 0.6, 0.6) \in S^M$ but $(0.6, 0.6, 0.6) \notin S^G$. To

show $S^U_{LP} \subseteq S^G_{LP}$ can be strict, the solution $(0.5, 0.5, 0.75) \in S^G_{LP}$ for $\lambda_{1,1} = \lambda_{1,2} = 0.5$, but $(0.5, 0.5, 0.75) \notin S^U_{LP}$. ■

Proposition 1 shows that the set we propose, S^U, is a tighter relaxation of S than those available in the literature (i.e., $S \subset S^U \subset S^G$ and $S^U_{LP} \subset S^G_{LP}$) and, further, that its linear programming relaxation is as tight as possible (i.e., $\text{conv}(S) = S^M = S^U_{LP}$), where $\text{conv}(S) = S^M$ is established in Al-Khayyal and Falk (1983). In our context, the value of Proposition 1 is that the set S captures how bilinear terms are treated in model $(\mathcal{P})$, and sets S^U, S^G, and S^M capture how we relax the bilinear terms in models $(\mathcal{U})$, $(\mathcal{G})$, and $(\mathcal{M})$, respectively. Section 4 investigates the computational advantage offered by the tighter model $(\mathcal{U})$.

3.3. Application to Microgrid Design and Dispatch Problem

We adopt the most precise battery modeling paradigm of which the authors are aware (Scioletti et al. 2016), wherein two sets of physical constraints in the microgrid design and dispatch problem include bilinear terms: (i) the battery power output (input) at each time period is the product of outgoing (incoming) current and voltage, which, in turn, is a linear function of battery state-of-charge; and, (ii) battery degradation is modeled as a function of current and state-of-charge. Hence, the product of battery state-of-charge and incoming or outgoing current at each time period comprise all the bilinear terms in the formulation of $(\mathcal{P})$ because this accounts for both the battery's power and lifecycle degradation. The model we adopt presents the round-trip energy losses as a function of the depth of a given charge-discharge cycle, which informs the voltage differential between the charge and discharge of the battery. This differs from most battery models in the literature, which approximate efficiency losses using a piece-wise linear function of battery charge or discharge power (Madathil et al. 2018), or via a constant efficiency loss to charge and/or discharge power (see, e.g., Felder and Hiskens 2014, Hari et al. 2018). We apply an additional, fixed efficiency loss to battery power output and input, which are noted in the Online Supplement in equations (15a) and (18c), respectively.

The graph in Figure 3 displays the bilinear terms in model $(\mathcal{P})$ for a particular battery technology; the indices that denote the battery technology and twin are shown in the Online Supplement, but are removed here for simplicity. For each time period t, the battery's starting state-of-charge, B^{soc}_{t-1}, shares a bilinear term with the charge and discharge current, denoted by I^+_t and I^-_t, respectively. The graph is bipartite, which suggests three

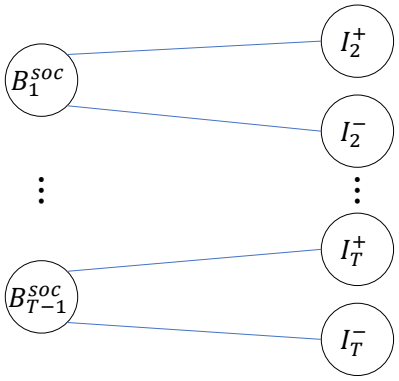

Figure 3: Graph displaying variables in bilinear terms in model ($\mathcal{P}$) for a particular battery technology; an edge between two nodes indicates that the corresponding variables comprise a bilinear term. For each period t, B_{t-1}^{soc} denotes the battery's starting state-of-charge, and I_t^+ and I_t^-, respectively, denote the current charging and discharging the battery. See the Online Supplement for details including equations (14), (18a), and (18b).

options for partitioning: (i) only partition on state-of-charge variables; (ii) only partition on current variables; or, (iii) partition on all variables. In Section 5.4, we investigate these three options. Next, we show the compact formulation for option (ii), which partitions one variable in each bilinear term and empirically results in better solution times than the other two options; see Section 5.4.

We use $|\mathcal{M}|$ and $|\mathcal{N}|$ to denote the number of partitions for each state-of-charge variable and each current charge and discharge variable, respectively. We map Y_{1t} to the starting state-of-charge and Y_{2t} to the current discharged from the battery in each time period, and we have an analogous pairing for the state-of-charge and current used to charge the battery. Under option (ii) from above, we partition only on Y_{2t} to obtain the following special case of model ($\mathcal{U}$):

$$\sum_{n\in\mathcal{N}} \lambda_{nt} = 1, \quad \forall t \in \mathcal{T} \tag{8a}$$

$$Y_{2t} \geq l_2 + (l_{2n} - l_2)\lambda_{nt}, \quad \forall n \in \mathcal{N}, t \in \mathcal{T} \tag{8b}$$

$$Y_{2t} \leq u_2 - (u_2 - u_{2n})\lambda_{nt}, \quad \forall n \in \mathcal{N}, t \in \mathcal{T} \tag{8c}$$

$$Z_t \geq u_{2n}Y_{1t} + u_1 Y_{2t} - u_1 u_{2n} - (u_1 - l_1)(u_2 - u_{2n})(1 - \lambda_{nt}), \quad \forall n \in \mathcal{N}, t \in \mathcal{T} \tag{8d}$$

$$Z_t \geq l_{2n}Y_{1t} + l_1 Y_{2t} - l_1 l_{2n} - (u_1 - l_1)(l_{2n} - l_2)(1 - \lambda_{nt}), \quad \forall n \in \mathcal{N}, t \in \mathcal{T} \tag{8e}$$

$$Z_t \leq l_{2n}Y_{1t} + u_1 Y_{2t} - u_1 l_{2n} + (u_1 - l_1)(l_{2n} - l_2)(1 - \lambda_{nt}), \quad \forall n \in \mathcal{N}, t \in \mathcal{T} \tag{8f}$$

$$Z_t \leq u_{2n}Y_{1t} + l_1 Y_{2t} - l_1 u_{2n} + (u_1 - l_1)(u_2 - u_{2n})(1 - \lambda_{nt}), \quad \forall n \in \mathcal{N}, t \in \mathcal{T} \tag{8g}$$

$$\lambda_{nt} \in \{0, 1\}, \quad \forall n \in \mathcal{N}, t \in \mathcal{T}. \tag{8h}$$

Constraints (8) are the special case of constraints (5) in which $|\mathcal{M}| = 1$; hence, we have removed index m and only use simple bounds l_1 and u_1 in our application. The formulation in the Online Supplement details the mappings of Y_{1t}, Y_{2t}, and Z_t to the state-of-charge and current decision variables in the microgrid design and dispatch problem.

4. Decomposition of MIP Formulation

While the approach we describe in Section 3 reduces approximation error compared to a McCormick linearization, the additional variables and constraints may compromise tractability. Because models $(\mathcal{P})$, $(\mathcal{U})$, $(\mathcal{G})$, and $(\mathcal{M})$ are loosely coupled with respect to time, a temporal decomposition can expedite computation. Rockafellar and Wets (1991) present the progressive hedging algorithm, which couples a Lagrangian relaxation of nonanticipativity constraints with a proximal term. Gade et al. (2016) and Escudero et al. (2016) both form lower bounds on the optimal value of multi-stage stochastic programs through Lagrangian relaxations of (subsets of) nonanticipativity constraints. This section introduces our approach to decomposing a larger problem into subproblems that can be solved in parallel to obtain upper and lower bounds on each model. While our approach can be applied to any of $(\mathcal{P})$, $(\mathcal{U})$, $(\mathcal{G})$, and $(\mathcal{M})$, for simplicity, we frame the discussion in terms of problem $(\mathcal{P})$, and we refer to the modified models that yield upper and lower bounds as $(\bar{\mathcal{P}})$ and $(\underline{\mathcal{P}})$, respectively.

The decomposition procedure begins by exploiting the time blocks indexed by $\ell \in \mathcal{L}$ in model $(\mathcal{P})$ to create a subproblem of the model for each interval. We create a clone of each strategic decision variable in each subproblem, and we introduce nonanticipativity constraints that force all subproblem strategic decisions to be equal. Next, we obtain a lower bound by relaxing the nonanticipativity constraints. We then obtain an upper bound by selecting and fixing a specific strategic decision, including the inventory level on the boundaries of each block. Updating the Lagrange multipliers associated with the relaxed nonanticipativity constraints tightens the lower bound, and we propose an updating scheme that performs well when applied to the microgrid design and dispatch problem.

4.1. $(\underline{\mathcal{P}})$ Formulation: Lower Bounds

To decompose model $(\mathcal{P})$ into $|\mathcal{L}|$ subproblems that together provide a lower bound on $(\mathcal{P})$, we start by allowing separate strategic decisions, X and R, per subproblem, and rewriting model $(\mathcal{P})$ as follows, in which we define μ^ℓ and θ^ℓ as dual variables for the nonanticipativity

constraints on X and R, respectively. (Typically, nonanticipativity constraints prevent decision variables from adapting to individual scenarios in a stochastic program. Here, they prevent strategic decisions from adapting to individual time blocks, ℓ.)

Additional Sets

$\mathcal{T}_\ell^-$ time periods in block ℓ, excluding the first period; i.e.,

$$\mathcal{T}_\ell^- = \mathcal{T}_\ell \setminus \{(\ell-1)\upsilon + 1\},\ \forall \ell \in \mathcal{L}$$

Additional Decision Variables

X^ℓ strategic design decision for subproblem ℓ

R^ℓ strategic inventory reset level for subproblem ℓ

Formulation

$$z^P = \min_{X, X^\ell, R, R^\ell, Y, \underline{Y}, \bar{Y}} \frac{1}{|\mathcal{L}|} \sum_{\ell \in \mathcal{L}} \left(f_0(X^\ell) + \sum_{\ell \in \mathcal{L}} \sum_{t \in \mathcal{T}_\ell} f_t(Y_t) \right. \tag{9a}$$

$$\text{s.t.} \quad X^\ell \in \mathcal{X}, \forall \ell \in \mathcal{L} \tag{9b}$$

$$Y_t \in \mathcal{Y}_t(X^\ell), \quad \forall t \in \mathcal{T}_\ell, \ell \in \mathcal{L} \tag{9c}$$

$$\bar{Y}_t = \underline{Y}_t + g_t(Y_t), \quad \forall t \in \mathcal{T} \tag{9d}$$

$$\underline{Y}_t = \bar{Y}_{t-1}, \quad \forall t \in \mathcal{T}_\ell^-, \ell \in \mathcal{L} \tag{9e}$$

$$\underline{Y}_{(\ell-1)\cdot\upsilon+1} = R^\ell, \quad \forall \ell \in \mathcal{L} \setminus \{1\} \tag{9f}$$

$$\bar{Y}_{\ell \cdot \upsilon} = R^\ell, \quad \forall \ell \in \mathcal{L} \tag{9g}$$

$$X^\ell = X, \quad \forall \ell \in \mathcal{L} : [\mu^\ell] \tag{9h}$$

$$R^\ell = R, \quad \forall \ell \in \mathcal{L} : [\theta^\ell] \tag{9i}$$

$$\underline{Y}_1 = Y_0 \tag{9j}$$

Model (9) clones the strategic decisions X and R via X^ℓ and R^ℓ, respectively, but enforces nonanticipativity constraints (9h) and (9i), and hence is equivalent to $(\mathcal{P})$ as specified in model (1). The objective function in (9a) is modified to incorporate the new X^ℓ variables. Constraints (9b)-(9d) replicate those of (1b)-(1d), when the nonanticipativity constraint (9h) is included. Constraint (9e) captures the inventory constraint (1e) for time

periods within a block, i.e., for $t \in \mathcal{T}_\ell^-,\ \ell \in \mathcal{L}$. Constraints (9f) and (9g), along with constraint (9i), maintain inventory across time blocks. Below, we use the dual variables indicated on constraints (9h) and (9i) to develop a Lagrangian relaxation of model (9). We refer to the following model as $(\underline{\mathcal{P}})$ because it provides a lower bound on model $(\mathcal{P})$'s optimal value.

$(\underline{\mathcal{P}})$ Formulation

$$\underline{z}^P = \min_{X^\ell, R^\ell, Y, \underline{Y}, \bar{Y}} \frac{1}{|\mathcal{L}|} \sum_{\ell \in \mathcal{L}} \Bigg(f_0(X^\ell) + \sum_{\ell \in \mathcal{L}} \sum_{t \in \mathcal{T}_\ell} f_t(Y_t) + \sum_{\ell \in \mathcal{L}} \Big(\mu^\ell X^\ell + \theta^\ell R^\ell \Big) \tag{10a}$$

$$\text{s.t.} \quad X^\ell \in \mathcal{X}, \quad \forall \ell \in \mathcal{L} \tag{10b}$$

$$Y_t \in \mathcal{Y}_t(X^\ell), \quad \forall t \in \mathcal{T}_\ell, \ell \in \mathcal{L} \tag{10c}$$

$$\bar{Y}_t = \underline{Y}_t + g_t(Y_t), \quad \forall t \in \mathcal{T} \tag{10d}$$

$$\underline{Y}_t = \bar{Y}_{t-1}, \quad \forall t \in \mathcal{T}_\ell^-, \ell \in \mathcal{L} \tag{10e}$$

$$\underline{Y}_{(\ell-1)\cdot v+1} = R^\ell, \quad \forall \ell \in \mathcal{L} \setminus \{1\} \tag{10f}$$

$$\bar{Y}_{\ell \cdot v} = R^\ell, \quad \forall \ell \in \mathcal{L} \tag{10g}$$

$$\underline{Y}_1 = Y_0 \tag{10h}$$

We require $\sum_{\ell \in \mathcal{L}} \mu^\ell = 0$ and $\sum_{\ell \in \mathcal{L}} \theta^\ell = 0$ to avoid an unbounded Lagrangian relaxation, which eliminates the free variables X and R. We can compute the lower bound of model (10), $\underline{z}^P$, by separating model $(\underline{\mathcal{P}})$ into $|\mathcal{L}|$ subproblems, one for each time block indexed by $\ell \in \mathcal{L}$. Proposition 2 shows that the optimal value of $(\underline{\mathcal{P}})$ provides a lower bound on model $(\mathcal{P})$, and extends the reformulation to create models $(\underline{\mathcal{U}})$, $(\underline{\mathcal{G}})$, and $(\underline{\mathcal{M}})$ to form lower bounds on models $(\mathcal{U})$, $(\mathcal{G})$, and $(\mathcal{M})$, respectively. The proposition further specifies relationships among these models.

PROPOSITION 2. *Let z^P, z^U, z^G, and z^M be the optimal values of $(\mathcal{P})$, $(\mathcal{U})$, $(\mathcal{G})$, and $(\mathcal{M})$, respectively. Similarly, let $\underline{z}^P$, $\underline{z}^U$, $\underline{z}^G$, and $\underline{z}^M$ be the optimal values of models $(\underline{\mathcal{P}})$, $(\underline{\mathcal{U}})$, $(\underline{\mathcal{G}})$, and $(\underline{\mathcal{M}})$, i.e., of model* (10) *specialized to the bilinear representation, or linear outer-approximation, under $(\mathcal{P})$, $(\mathcal{U})$, $(\mathcal{G})$, and $(\mathcal{M})$, respectively. Then, $z^P \geq \underline{z}^P$, $z^U \geq \underline{z}^U$, $z^G \geq \underline{z}^G$, $z^M \geq \underline{z}^M$, and $z^P \geq z^U \geq z^G \geq z^M$. Further, assume that the same multipliers $\mu^\ell, \theta^\ell,\ \forall \ell \in \mathcal{L}$, are used in models $(\underline{\mathcal{P}})$, $(\underline{\mathcal{U}})$, $(\underline{\mathcal{G}})$, and $(\underline{\mathcal{M}})$. Then, $\underline{z}^P \geq \underline{z}^U \geq \underline{z}^G \geq \underline{z}^M$.*

Proof. Model $(\mathcal{P})$ as defined in (1) is equivalent to model (9), and model $(\underline{\mathcal{P}})$ as defined in (10) is a Lagrangian relaxation of (9) under the restriction on the multipliers of

$\sum_{\ell\in\mathcal{L}}\mu^\ell = 0$ and $\sum_{\ell\in\mathcal{L}}\theta^\ell = 0$. Thus, $z^P \geq \underline{z}^P$. An analogous argument shows that $z^U \geq \underline{z}^U$, $z^G \geq \underline{z}^G$, and $z^M \geq \underline{z}^M$. Using Proposition 1, we have $z^M \leq z^G \leq z^U \leq z^P$, and $\underline{z}^M \leq \underline{z}^G \leq \underline{z}^U \leq \underline{z}^P$. ■

4.2. ($\bar{\mathcal{P}}$) Formulation: Upper Bounds

We make two modifications to model (9) to obtain an upper bound on ($\mathcal{P}$)'s optimal value, and call the resulting model ($\bar{\mathcal{P}}$). First, we fix a design decision $\hat{X} \in \mathcal{X}$, and second, we fix a "reset point" for inventory levels at boundaries of the partition on $\mathcal{T}$, which we call $\hat{R}$. We obtain as many as $|\mathcal{L}|$ candidate solutions by solving ($\underline{\mathcal{P}}$), and we may select one of these; our implementation retrieves candidates from peak demand intervals and retains that which provides the tightest upper bound upon solving ($\bar{\mathcal{P}}$).

($\bar{\mathcal{P}}$) Formulation

$$\bar{z}^P = \min_{Y,\underline{Y},\bar{Y}} \; f_0(\hat{X}) + \sum_{\ell\in\mathcal{L}}\sum_{t\in\mathcal{T}_\ell} f_t(Y_t) \tag{11a}$$

$$\text{s.t.} \;\; Y_t \in \mathcal{Y}_t(\hat{X}), \quad \forall t \in \mathcal{T}_\ell, \ell \in \mathcal{L} \tag{11b}$$

$$\bar{Y}_t = \underline{Y}_t + g_t(Y_t), \quad \forall t \in \mathcal{T} \tag{11c}$$

$$\underline{Y}_t = \bar{Y}_{t-1}, \quad \forall t \in \mathcal{T}_\ell^-, \ell \in \mathcal{L} \tag{11d}$$

$$\underline{Y}_{(\ell-1)\cdot v+1} = \hat{R}, \quad \forall \ell \in \mathcal{L}\setminus\{1\} \tag{11e}$$

$$\bar{Y}_{\ell\cdot v} = \hat{R}, \quad \forall \ell \in \mathcal{L} \tag{11f}$$

$$\underline{Y}_1 = Y_0 \tag{11g}$$

Fixing the design decision at $\hat{X}$ and inventory reset value at $\hat{R}$ allows for the removal of constraints (9b), (9h) and (9i). The boundary conditions (11e) and (11f) link the pairs of decision variables $\underline{Y}$ and $\bar{Y}$ that span multiple intervals within the partition on $\mathcal{T}$ by fixing their values to the reset point $\hat{R}$; these replace constraint (9i), and allow model (11) to separate by $\ell \in \mathcal{L}$. The optimal value of ($\bar{\mathcal{P}}$) provides an upper bound on the optimal value of ($\mathcal{P}$), per Proposition 3.

Proposition 3. *Let $\hat{X} \in \mathcal{X}$ and $\hat{R}$ be given, and assume that for those $\hat{X}$ and $\hat{R}$, model ($\bar{\mathcal{P}}$) is feasible. Let z^P, z^U, z^G, and z^M be the optimal values of ($\mathcal{P}$), ($\mathcal{U}$), ($\mathcal{G}$), and ($\mathcal{M}$), respectively. Similarly, let $\bar{z}^P$, $\bar{z}^U$, $\bar{z}^G$, and $\bar{z}^M$ be the optimal values of models ($\bar{\mathcal{P}}$), ($\bar{\mathcal{U}}$), ($\bar{\mathcal{G}}$), and ($\bar{\mathcal{M}}$), i.e., of model* (11) *specialized to the bilinear representation, or linear outer-approximation, under ($\mathcal{P}$), ($\mathcal{U}$), ($\mathcal{G}$), and ($\mathcal{M}$), respectively. Then, $\bar{z}^P \geq z^P$, $\bar{z}^U \geq z^U$, $\bar{z}^G \geq z^G$, and $\bar{z}^M \geq z^M$. Further, $\bar{z}^P \geq \bar{z}^U \geq \bar{z}^G \geq \bar{z}^M$.*

Proof. By Proposition 1, feasibility of $(\bar{\mathcal{P}})$ ensures feasibility of $(\bar{\mathcal{U}})$, $(\bar{\mathcal{G}})$, and $(\bar{\mathcal{M}})$ under $\hat{X}$ and $\hat{R}$. Consider models $(\bar{\mathcal{P}})$ as defined in (11) and $(\mathcal{P})$ as re-expressed in (9). Boundary conditions (11e) and (11f) are equivalent to constraints (9f) and (9g), except that the inventory variable $R = \hat{R}$ has been fixed. Additionally, the design decision $X = \hat{X} \in \mathcal{X}$ is fixed. Therefore, $(\bar{\mathcal{P}})$ is a restriction of $(\mathcal{P})$, and hence its optimal value yields an upper bound for $(\mathcal{P})$; i.e., $\bar{z}^P \geq z^P$. Analogous arguments show $\bar{z}^U \geq z^U$, $\bar{z}^G \geq z^G$, and $\bar{z}^M \geq z^M$. Using Proposition 1, we have $\bar{z}^P \geq \bar{z}^U \geq \bar{z}^G \geq \bar{z}^M$. ■

4.3. Decomposition Algorithm

Algorithm 1 iteratively improves the solutions to the lower and upper bounding formulations in Sections 4.1 and 4.2, respectively, tightening the bounds as the algorithm proceeds. For simplicity, we describe the algorithm as applied to a generic model, $(\mathcal{A})$, but it may be applied to any of $(\mathcal{P})$, $(\mathcal{U})$, $(\mathcal{G})$, and $(\mathcal{M})$. Additionally, valid mixtures according to Propositions 2 and 3 are possible; for example, we may use $(\bar{\mathcal{P}})$=$(\bar{\mathcal{A}})$ and $(\underline{\mathcal{U}})$=$(\underline{\mathcal{A}})$ to obtain upper and lower bounds on model $(\mathcal{P})$=$(\mathcal{A})$.

To obtain ε-optimal solutions to model $(\mathcal{A})$, we iteratively solve models $(\underline{\mathcal{A}})$ and $(\bar{\mathcal{A}})$ using a variation of the progressive hedging method developed by Rockafellar and Wets (1991). Let X_0 and R_0 denote a design decision and an inventory level, respectively, obtained by selecting a candidate from solutions to the subproblems of model $(\mathcal{A})$. Then, Algorithm 1 aims to iteratively improve upper and lower bounds on the optimal value of the model, which we call z^A, until we obtain a solution whose optimality gap is within the desired tolerance.

Each iteration in Algorithm 1 updates Lagrange multipliers θ^ℓ according to step-size parameters ρ_θ, the distance between each reset inventory level R^ℓ, and its time-weighted mean value; we update multipliers μ^ℓ using ρ_μ and X^ℓ under an analogous method. Algorithm 1 is similar to progressive hedging, but in solving $(\underline{\mathcal{A}})$ we do not include a proximal term in the objective function; therefore, solving $(\underline{\mathcal{A}})$ provides a valid lower bound for z^A at every iteration. Figure 4 displays the key outputs of each model under our approach.

4.4. Application to a Microgrid Design and Dispatch Problem

In what follows, we detail our methodology to formulate, and update, models that bound $(\mathcal{P})$ specific to the microgrid design and dispatch problem developed by Scioletti et al. (2017). We use multiple models from this paper to approximate $(\mathcal{P})$, and we solve

Algorithm 1 Decomposition procedure to approximately solve model $(\mathcal{A})$

procedure DECOMPOSITION

Inputs: $\varepsilon > 0, \rho_\mu > 0, \rho_\theta > 0, k \in \mathbb{Z}_+, \kappa \in \mathbb{Z}_+, (\underline{\mathcal{A}}), (\bar{\mathcal{A}})$ ▷ stopping criterion, ▷ proximal weights, upper bound search frequency, upper bound search depth, ▷ models to obtain lower and upper bounds

Outputs: $X^*, R^*, \bar{z}^A, \underline{z}^A$ ▷ ε-optimal design and inventory, ▷ upper and lower bounds on z^A

$i \leftarrow 0;\ \underline{z}^A \leftarrow -\infty;\ \bar{z}^A \leftarrow \infty$ ▷ iteration and initial lower and upper bounds

$\mu^\ell \leftarrow 0,\ \theta^\ell \leftarrow 0,\ \forall \ell \in \mathcal{L}$ ▷ initial Lagrange multipliers for model $(\underline{\mathcal{A}})$

while $\bar{z}^A - \underline{z}^A > \varepsilon \bar{z}^A$ **do**

Solve $(\underline{\mathcal{A}})$ with μ^ℓ, θ^ℓ to obtain $\underline{z}_i, X^\ell, R^\ell,\ \ell \in \mathcal{L}$ ▷ $\underline{z}_i$ is a lower bound for z^A ▷ $|\mathcal{L}|$ subproblems in $(\underline{\mathcal{A}})$ can be solved in parallel

$\bar{X} \leftarrow \frac{1}{|\mathcal{L}|} \sum_{\ell \in \mathcal{L}} X^\ell;\ \bar{R} \leftarrow \frac{1}{|\mathcal{L}|} \sum_{\ell \in \mathcal{L}} R^\ell$ ▷ mean of subproblem designs, reset inventories

for $\ell = 1, \ldots, |\mathcal{L}|$ **do** ▷ update Lagrange multipliers

$\mu^\ell \leftarrow \mu^\ell + \rho_\mu (X^\ell - \bar{X});\ \theta^\ell \leftarrow \theta^\ell + \rho_\theta (R^\ell - \bar{R})$

if $\underline{z}_i > \underline{z}^A$ **then** $\underline{z}^A \leftarrow \underline{z}_i$ ▷ update lower bound, if improved

if $i \bmod k = 0$ **then** ▷ attempt to find a new upper bound every k iterations

$j \leftarrow 0$

for $\ell \in \mathcal{L}$ **do**

if X^ℓ not previously used to solve $(\bar{\mathcal{A}})$ **then**

$j \leftarrow j + 1$

Solve $(\bar{\mathcal{A}})$ with $\hat{X} = X^\ell,\ \hat{R} = r(X^\ell)$ to obtain $\bar{z}_i^\ell$ ▷ $\bar{z}_i^\ell$ is an upper bound for z^A ▷ $r(X^\ell)$ is the midpoint of upper and lower bounds on R, given X^ℓ ▷ $|\mathcal{L}|$ subproblems in $(\bar{\mathcal{A}})$ can be solved in parallel

if $\bar{z}_i^\ell < \bar{z}^A$ **then** ▷ update upper bound and incumbent solution, ▷ if improved

Solve $(\bar{\mathcal{A}})$ with $\hat{X} = X^\ell$, optimizing R via bisection search to obtain R^ℓ, $\bar{z}_i^\ell$

$X^* \leftarrow X^\ell,\ R^* \leftarrow R^\ell,\ \bar{z}^A \leftarrow \bar{z}_i^\ell$

if $\bar{z}^A - \underline{z}^A \le \varepsilon \bar{z}^A$ **or** $j = \kappa$ **then end-for**

$i \leftarrow i + 1$

return $(X^*, R^*, \bar{z}^A, \underline{z}^A)$

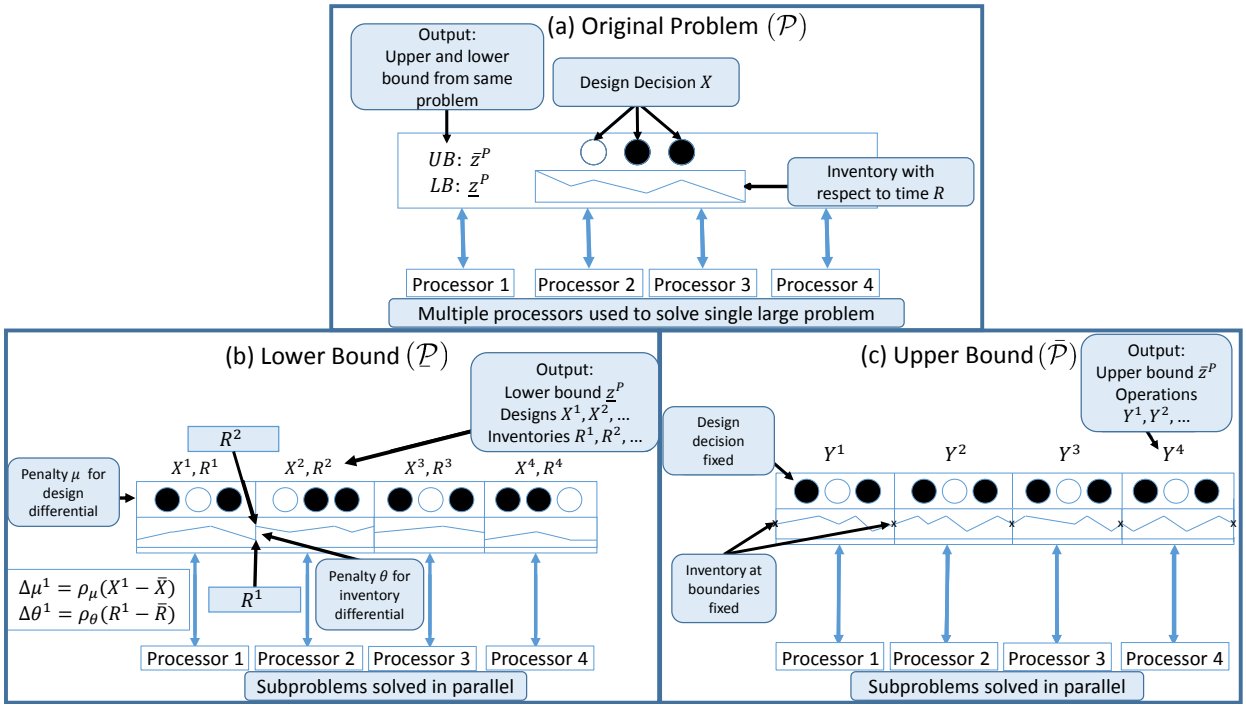

Figure 4: Illustration of direct solution of $(\mathcal{P})$ and Algorithm 1 applied to $(\mathcal{A})$=$(\mathcal{P})$. Part (a) of the figure depicts how a general purpose MINLP solver would solve model $(\mathcal{P})$. The bounds $\underline{z}$ and $\bar{z}$ are from a branch-and-bound algorithm, and that algorithm could use multiple processors. Based on Algorithm 1, part (b) shows the reconciliation of the subproblems of $(\mathcal{P})$, while part (c) shows that of the subproblems of $(\bar{\mathcal{P}})$.

these via Algorithm 1. Specifically, we use a mixture of $(\bar{\mathcal{P}})$ and $(\mathcal{U})$ to obtain upper and lower bounds, respectively.

4.4.1. Tightening $(\mathcal{U})$ via a lower bound on generator capacity. Design decisions chosen for subproblems in off-peak time periods may be infeasible to the year-long problem due to insufficient generator capacity. To address this and to tighten the lower bound obtained by solving $(\mathcal{U})$, we develop and solve a variant of model $(\mathcal{U})$ in which in each subproblem we minimize the sum of the capacities of all diesel generators selected in the optimal design. That is, we seek a feasible solution to each subproblem that uses the smallest possible total generator capacity. The maximum of the optimal objective function values, i.e., the sum of the generator capacities, from these subproblems is then used to form a valid inequality, setting a lower bound on diesel generator capacity when iteratively solving model $(\mathcal{U})$ in Algorithm 1. Enforcing this minimum generator capacity strengthens constraints (10b)-(10c) for periods in which average and peak loads are low relative to those over the time horizon.

4.4.2. Obtaining feasible solutions to model $(\mathcal{P})$, using solutions to model $(\mathcal{U})$. We exploit the limited approximation error associated with model $(\mathcal{U})$ to develop solutions

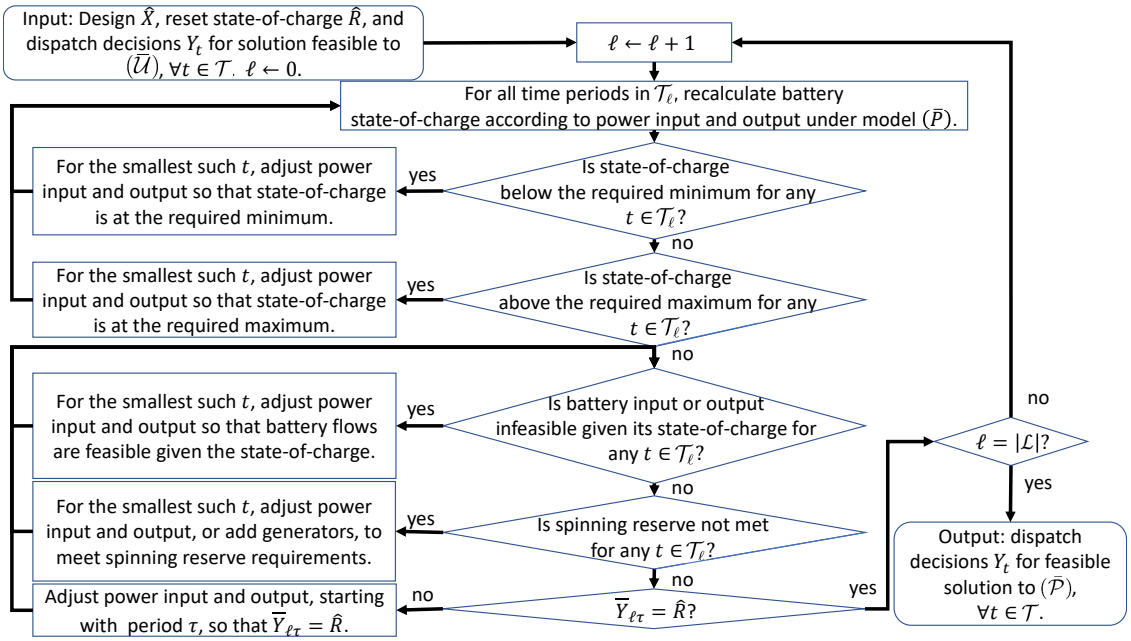

Figure 5: Flowchart describing procedure to find a feasible solution to $(\mathcal{P})$, using a solution to $(\mathcal{U})$ as a starting point.

feasible to the nonlinear model $(\mathcal{P})$ by using a solution to model $(\mathcal{U})$ as input. The flowchart in Figure 5 details the heuristic for obtaining such a solution. For each subproblem ℓ, the heuristic enforces the nonlinear constraints of model $(\mathcal{P})$ and recalculates battery state-of-charge for each time period in the subproblem, using the battery power from the optimized dispatch decisions from model $(\mathcal{U})$. Then, the heuristic turns diesel generators on or off and adjusts their power output until the battery power input and output are feasible to $(\mathcal{P})$ for each period $t \in \mathcal{T}_\ell$.

5. Computational Results

In this section, we first briefly describe the collection of 14 problem instances from Scioletti et al. (2017). Then, we report computational results for these instances under the partitioning scheme for bilinear terms from Section 3 and the decomposition algorithm of Section 4. The results: (i) demonstrate the benefit of Algorithm 1 by comparing the time to solve the McCormick relaxation model $(\mathcal{M})$ using our method to that of solving model $(\mathcal{M})$ directly; (ii) exhibit the improvements due to our tightened linearization of bilinear terms by comparing results of our model $(\mathcal{U})$ and that of Gounaris et al. $(\mathcal{G})$; (iii) validate the use of a partitioning scheme by using solutions to $(\mathcal{U})$ as a starting point to obtain an upper bound on the nonlinear model $(\mathcal{P})$; and, (iv) detail the impact of the problem-specific methods from Sections 3.3 and 4.4 on solution quality by comparing

the bounds on ($\mathcal{U}$) achieved under subsets of these ideas. For all MIP instances, we used CPLEX v. 12.6.2.0 (IBM 2017) to either solve the model directly or to solve subproblems from our decomposition algorithm. Our implementation of Algorithm 1 is in Python 2.7.9 (Rossum 1995), and all results were obtained on a Cray XC40 compute node with two Intel E5-2690 v3 12-core (Haswell) processors and 64 GB of DDR4 memory.

5.1. Load and Candidate Design Technologies

Forward Operating Bases (FOBs) serve as protected locations from which to project and sustain combat operations, require significant logistical support, and must produce electrical power without a connection to the grid. While FOBs, or in general, the population and land mass of any remote site, vary greatly in size and location, we obtained data for remote locales with no more than 150 soldiers residing within a 100m by 100m area, with peak power load of at most 300kW over an operating time horizon of one year. This section outlines the source of load and candidate storage and generation assets for our model instances.

The FOB demand profiles were simulated in EnergyPlus (2001), based on an experiment conducted at the Basecamp Integration Lab at Fort Devens, MA. The four diesel generator technologies we consider are currently available in the military inventory, and have power ratings from 15kW to 100kW, with purchase costs between \$25K and \$38K. The lone type of PV system we consider is assumed to have fixed-tilt-and-angle panels with a nameplate rating of 1kW; we assume that spatial restrictions impose a limit of 75 such systems, at a purchase cost of \$2/W. The battery technologies that we consider are sourced from A123 (2018) and have a purchase cost of \$500/kWh, with a minimum of one hour for a full discharge and three hours for a full charge.

5.2. Solution of Model ($\mathcal{M}$) via Decomposition

We demonstrate the benefit of using Algorithm 1 to solve model ($\mathcal{M}$), over solving ($\mathcal{M}$) directly. Table 1 displays solution times and optimality gaps for our 14 test problems; the decomposition procedure outperforms direct solution in each instance, decreasing the solution time from a minimum of 56 minutes for the direct solution procedure to a maximum of six minutes for Algorithm 1.

	Algorithm 1, $\lvert\mathcal{L}\rvert$=365				Direct Solution	
Instance	$\underline{z}^M$ **($MM)**	$\bar{z}^M$ **($MM)**	**Gap (%)**	**Solve Time (seconds)**	**Gap (%)**	**Solve Time (seconds)**
Bagram	1.961	2.031	3.53	285	4.96	15,333
Bamako	1.016	1.050	3.41	52	4.40	8,684
Brazzaville	1.241	1.249	0.70	44	4.06	7,155
Buenos Aires	1.591	1.631	2.50	94	6.67	18,000
Dili	1.438	1.448	0.71	66	4.17	9,273
Dushanbe	2.113	2.166	2.52	328	8.08	18,000
Boston	3.401	3.466	1.92	222	7.43	18,000
Gengneung	2.520	2.575	2.15	195	6.81	18,000
Istanbul	2.157	2.200	2.01	154	8.39	18,000
Kuwait City	1.627	1.702	4.59	146	10.13	18,000
Mexico City	1.127	1.157	2.66	119	9.61	18,000
San Salvador	0.967	0.974	0.76	52	4.53	3,333
Tallinn	2.567	2.620	2.08	190	9.95	18,000
Springfield	3.885	3.978	2.38	245	4.97	11,746

Table 1: Computational results for a collection of year-long ($\lvert\mathcal{T}\rvert$ =8,760) instances of model ($\mathcal{M}$). Models are solved using CPLEX v. 12.6.2.0, via Python 2.7.9.
• Termination criterion for "Algorithm 1" and "Direct Solution": min{time limit $\leq$ 5 hours, optimality gap $\leq$ 5%}.
• Termination criterion per subproblem: min{time limit $\leq$ 60 seconds, optimality gap $\leq$ 0.5%}; the 60-second time limit was reached in fewer than 1% of cases.

5.3. Solution of Model ($\mathcal{U}$) vs. Model ($\mathcal{G}$)

We illustrate the impact of our tighter mixed integer linear relaxation, ($\mathcal{U}$), compared to that of Gounaris et al. (2009), ($\mathcal{G}$), by using Algorithm 1 to solve each formulation over the 14 instances. Proposition 1 shows that these problems share the same set of feasible solutions when the binary restrictions in constraint (8h) hold; however, when this constraint is relaxed, the tighter model ($\mathcal{U}$) allows us to obtain high-quality lower bounds more quickly. Table 2 compares the solution times from applying Algorithm 1 to models ($\mathcal{U}$) and ($\mathcal{G}$), as well as another formulation discussed in Nagarajan et al. (2019), which we denote ($\mathcal{N}$), all using the same tolerance of a 5% optimality gap. Using our tighter relaxation reduces solution times by about 20%, on average, relative to those obtained from model ($\mathcal{G}$), and reaches a 5% tolerance in the shortest amount of time of the three models in each instance.

All three models use $|\mathcal{M}| = 1$ (state-of-charge) and $|\mathcal{N}| = 4$ (current) uniform subregions. Unlike our model ($\mathcal{U}$), the model of Nagarajan et al. (2019) does not achieve the convex hull, but its number of binary variables scales with $|\mathcal{M}| + |\mathcal{N}|$ rather than our $|\mathcal{M}| \cdot |\mathcal{N}|$. The lower running times for ($\mathcal{U}$) versus ($\mathcal{N}$) may be due to the fact that we can achieve a 5% gap more quickly by simply using univariate partitioning, i.e., $|\mathcal{M}| = 1$ in our application. We further discuss this choice of $|\mathcal{M}|$ and $|\mathcal{N}|$ in Section 5.4; see also Section 3.3.

	Time to reach 5% tolerance (seconds)		
Instance	($\mathcal{U}$)	($\mathcal{G}$)	($\mathcal{N}$)
Bagram	671	882	1,858
Bamako	438	451	932
Brazzaville	235	260	331
Buenos Aires	318	339	431
Dili	358	365	572
Dushanbe	827	1,120	3,206
Boston	453	532	622
Gengneung	871	1,375	2,883
Istanbul	257	463	2,482
Kuwait City	510	520	914
Mexico City	318	387	479
San Salvador	221	224	346
Tallinn	261	305	355
Springfield	585	652	2,231

Table 2: Computational results of using Algorithm 1 to approximately solve instances of models ($\mathcal{U}$) ($\mathcal{G}$), and model (4) from Nagarajan et al. (2019), which we denote ($\mathcal{N}$). Here, $|\mathcal{T}| = 8{,}760$ hrs, $|\mathcal{L}| = 365$, and we use $|\mathcal{M}| = 1$ (state-of-charge) and $|\mathcal{N}| = 4$ (current) uniform subregions in all three approaches.
Models are solved using CPLEX v. 12.6.2.0, via Python 2.7.9.
• Termination criterion for Algorithm 1: optimality gap $\leq 5\%$.
• Termination criterion per subproblem: min{time limit ≤ 60 seconds, optimality gap $\leq 0.5\%$}; the 60-second time limit was reached in fewer than 5% of cases.

5.4. Solution of Model ($\mathcal{P}$)

To obtain a feasible solution to the MINLP model ($\mathcal{P}$), we iteratively solve models ($\underline{\mathcal{U}}$) and ($\bar{\mathcal{U}}$), and then use the procedure in Figure 5 to obtain solutions to model ($\bar{\mathcal{P}}$). Table 3 displays the solution times and optimality gaps achieved on model ($\mathcal{P}$).

We obtain solutions within 5% of optimality within 20 minutes for all 14 MINLP instances, a significant result for the nonlinear microgrid design and dispatch problem using this set of technologies on year-long instances. For comparison, Scioletti et al. (2017) were unable to achieve 5% optimality gaps for day-long instances ($|\mathcal{T}| = 24$ hours) in the 14 locations within three hours, using any of the general-purpose MINLP solvers BARON (Sahinidis 1996), Bonmin (Bonami and Lee 2009), or Couenne (Belotti 2009), and for nine of the instances, they fail to obtain a feasible solution within three hours.

Instance	$\underline{z}^*$ ($MM)	$\bar{z}^*$ ($MM)	Gap (%)	Solve Time (seconds)
Bagram	1.963	2.062	5.00	877
Bamako	1.017	1.061	4.29	883
Brazzaville	1.244	1.268	1.92	443
Buenos Aires	1.594	1.651	3.63	522
Dili	1.442	1.466	1.69	563
Dushanbe	2.114	2.190	3.58	1,172
Boston	3.401	3.486	2.50	651
Gengneung	2.521	2.585	2.53	1,078
Istanbul	2.157	2.219	2.87	266
Kuwait City	1.629	1.698	4.29	837
Mexico City	1.129	1.176	4.20	525
San Salvador	0.969	0.992	2.31	426
Tallinn	2.568	2.635	2.62	476
Springfield	3.886	3.995	2.80	791

Table 3: Computational results of approximately solving MINLP model ($\mathcal{P}$) ($|\mathcal{T}|$ = 8,760 hrs, $|\mathcal{L}| = 365$).
Models ($\bar{\mathcal{U}}$) and ($\mathcal{U}$) are solved with $|\mathcal{M}| = 1$ (state-of-charge) and $|\mathcal{N}| = 4$ (current) uniform subregions using CPLEX v. 12.6.2.0, via Python 2.7.9. The second column ($\underline{z}^*$) reports the optimal value of ($\mathcal{U}$). The third column ($\bar{z}^*$) reports the objective function value of the feasible solution to model ($\bar{\mathcal{P}}$) obtained by adjusting solutions to model ($\bar{\mathcal{U}}$) via the procedure in Figure 5.
• Termination criterion for Algorithm 1: ($\mathcal{U}$) optimality gap $\leq$ 5%.
• Termination criterion per subproblem: min{time limit $\leq$ 60 seconds, optimality gap $\leq$ 0.5%}; the 60-second time limit was reached in fewer than 5% of cases.

We compare the performance related to different values for $|\mathcal{M}|$ and $|\mathcal{N}|$ in the partitioning scheme we use to create model ($\mathcal{U}$) by adopting two variants of the performance profile of Dolan and Moré (2002). In the first variant, we compare the optimality gaps

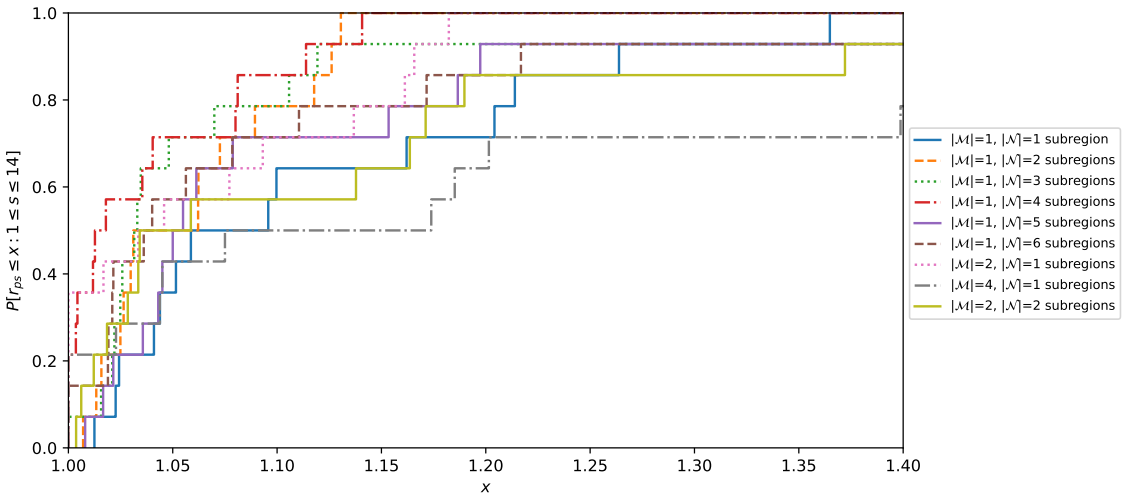

Figure 6: Performance profile for the partitioning scheme of model ($\mathcal{U}$) in which the number of subregions for battery state-of-charge, $|\mathcal{M}|$, and for current, $|\mathcal{N}|$, vary between one and four and one and six, respectively, for our 14 instances. Here, we solve models ($\mathcal{U}$) and ($\bar{\mathcal{U}}$) via Algorithm 1, and then use the procedure of Figure 5 to obtain solutions to ($\bar{\mathcal{P}}$). The value r_{ps} is calculated using equation (12). For $|\mathcal{M}| = 1$ and $|\mathcal{N}| = 4$, the performance profile reaches the value of 1.0 at $x = 1.141$, meaning that the algorithm with this partitioning scheme achieves a gap within 1.141 times the best gap for all nine choices of the partition across all 14 instances.

achieved for a one-hour time limit as the number of subregions in our partitioning scheme varies. Let g_{ps} be the optimality gap achieved in one hour of runtime using the p-th design for the subregions for instance s. Then, our performance ratio, r_{ps}, is defined as

$$r_{ps} = \frac{g_{ps}}{\min\limits_{p=1,\ldots,9}\{g_{ps}\}}. \tag{12}$$

Here, $p = 1, \ldots, 9$ ranges over the nine choices for designing the partition shown in Figure 6's legend. The figure displays the performance profile as a cumulative distribution function, using the 14 instances from our application as samples. The x-axis in Figure 6 specifies a multiplicative factor on the best optimality gap. So, with $|\mathcal{M}| = 1$ and $|\mathcal{N}| = 4$ subregions, we can solve 12 out of 14 instances within a factor of 1.08 of the best gap obtained by all nine partitioning schemes.

In our second variant of the performance profile from Dolan and Moré (2002), we report the optimality gaps achieved by each partitioning scheme as a function of time in the following manner. Let g_{pst} be the optimality gap achieved in t seconds of runtime using the p-th partitioning scheme to solve instance s. Then, our performance ratio at time t, r_{pst}, is defined as

$$r_{pst} = \frac{\min\limits_{p=1,\ldots,9}\{g_{ps\tau}\}}{g_{pst}}, \tag{13}$$

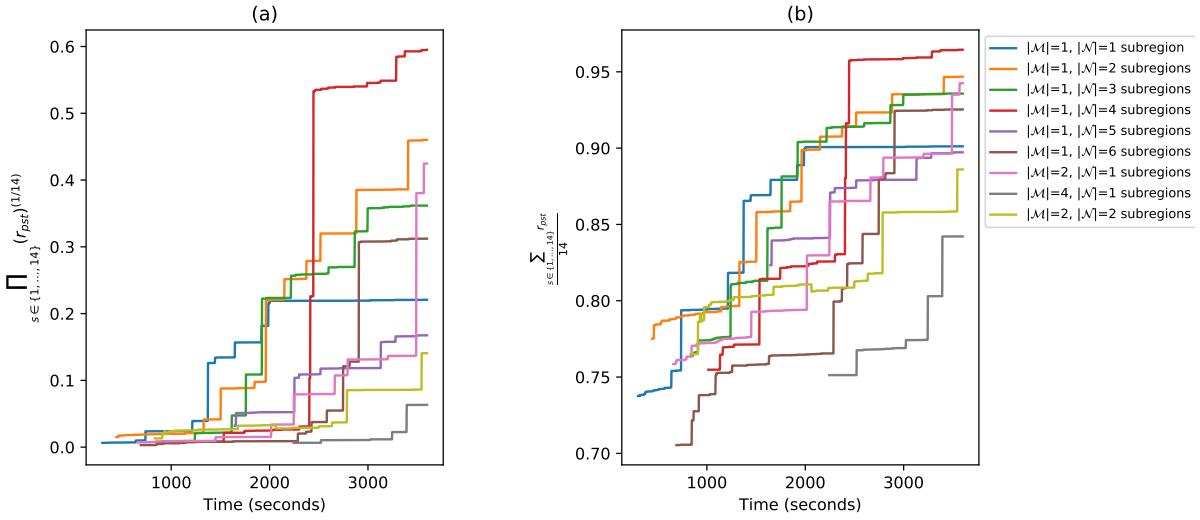

Figure 7: Performance profile of the metric r_{pst} over time for our partitioning scheme in which the number of subregions for battery state-of-charge, $|\mathcal{M}|$, and for current, $|\mathcal{N}|$, vary between one and four and one and six, respectively, for the 14 instances in our application. The value r_{pst} is calculated using equation (13). Part (a) and part (b) display the geometric and arithmetic means of r_{pst}, respectively. Here, we solve models ($\mathcal{U}$) and ($\bar{\mathcal{U}}$) via Algorithm 1, and then use the procedure of Figure 5 to obtain solutions to ($\bar{\mathcal{P}}$).

in which $\tau = 3,600$ seconds, the time limit for each instance.

Unlike the performance measure of equation (12), the measure in equation (13) tracks the optimality gap as a function of time. Both measures are constructed so that values "higher and to the left" indicate superior performance. Figure 7 displays the geometric and arithmetic means of r_{pst} across the 14 instances. While the partitioning scheme exhibits the tightest optimality gaps using $|\mathcal{M}| = 1$ and $|\mathcal{N}| = 4$ subregions for our collection of instances with a one-hour time limit, the results suggest that $|\mathcal{M}| = 1$ and $|\mathcal{N}| = 2$ subregions may provide tighter gaps under a stricter computational budget.

Table 4 details the impact of the problem-specific scheme we describe in Section 4.4.1 in which we add a constraint that provides a lower bound on diesel generator capacity. The table shows that this significantly reduces solution times when using Algorithm 1 to solve the nonlinear microgrid design and dispatch problem on our 14 instances.

5.5. Model Validation

Our model was validated using a hardware implementation in a separate effort by team of collaborators (Foy 2018) at MIT-Lincoln Laboratory (MIT-LL), who developed an algorithm that efficiently dispatches generators and energy storage to meet demand, plus a reserve for reliability, within certain hardware constraints (e.g., minimum on- and off-times,

	$(\bar{\mathcal{P}})$ and $(\mathcal{U})$ Only		Generator Capacity Valid Inequality	
Instance	**Gap (%)**	**Solve Time (seconds)**	**Gap (%)**	**Solve Time (seconds)**
Bagram	17.77	7,200	5.00	877
Bamako	5.51	7,200	4.29	883
Brazzaville	2.25	325	1.92	443
Buenos Aires	5.74	7,200	3.63	522
Dili	1.75	524	1.69	563
Dushanbe	5.36	7,200	3.58	1,172
Boston	3.98	7,184	2.50	651
Gangneung	3.73	620	2.53	1,078
Istanbul	4.26	2,824	2.87	266
Kuwait City	5.28	7,200	4.29	837
Mexico City	4.16	2,021	4.20	525
San Salvador	2.61	469	2.31	426
Tallinn	4.34	3,570	2.62	476
Springfield	5.57	7,200	2.80	791

Table 4: Computational results of approximately solving instances of MINLP model $(\mathcal{P})$ ($|\mathcal{T}| = 8{,}760$ hrs, $|\mathcal{L}| = 365$). Models $(\bar{\mathcal{U}})$ and $(\mathcal{U})$ are solved with $|\mathcal{M}| = 1$ (state-of-charge) and $|\mathcal{N}| = 4$ (current) uniform subregions using CPLEX v. 12.6.2.0, via Python 2.7.9. Solutions to model $(\bar{\mathcal{P}})$ were obtained by adjusting solutions to model $(\bar{\mathcal{U}})$ via the procedure in Figure 5. The right-most columns include the lower bound on required diesel generator capacity per Section 4.4.1.
• Termination criterion for Algorithm 1: min{time limit $\leq$ 2 hours, $(\mathcal{P})$ optimality gap $\leq 5\%$}.
• Termination criterion per subproblem: min{time limit $\leq$ 60 seconds, optimality gap $\leq 0.5\%$}; the 60-second time limit was reached in fewer than 5% of cases.

maximum loading, and ramping) for given sets of equipment similar to those we consider here. The logic in the algorithm implemented in the hardware tests mimics our heuristic policy (Figure 5); see also the similar heuristics of Scioletti et al. (2017) and Goodall et al. (2019). The algorithm responds to demand and the battery's state-of-charge, with dispatch decisions for the generators and storage, without knowledge of future demand. The MIT-LL team's algorithm is run in Simulink for a range of conditions, and used in multiple, successful field tests with various load profiles to demonstrate its ability to reduce fuel consumption over legacy (i.e., generator-only) configurations by 25%, which is similar to the results presented in Table 9 of Scioletti et al. (2017).

6. Summary and Future Work

This paper advances two integrated methods that take advantage of problems that are loosely coupled with respect to time and contain bilinear terms. For the latter issue, we develop a partitioning scheme that approximates bilinear terms. We show that our scheme achieves the requisite convex hull, and is a tighter relaxation than similar approaches in the literature, both in practice on our test problems and in theory. We present a decomposition method that separates the problem into smaller subproblems, using Lagrangian relaxation to obtain a lower bound and fixing inventory levels at regular intervals to obtain an upper bound. We apply the methodology to a microgrid design and dispatch problem, solve instances to within 5% of MIP optimality in at most six minutes, and achieve a 5% MINLP gap for all instances within 20 minutes, which significantly improves on alternative approaches.

Our microgrid design and dispatch problem could benefit from a model that more fully hedges against uncertainty in load and solar irradiance. While our model appears to have perfect information on these parameters over the course of a year, only the battery's state-of-charge links the model temporally. Our computation requires the state-of-charge to reset daily, and this limits foresight to 24 hours. Once the design variables—which procure generators, PV, batteries, and select the battery state-of-charge reset value—have been fixed, the model separates into $|\mathcal{L}| = 365$ daily dispatch models. This construct resembles a two-stage stochastic program in which we face $|\mathcal{L}|$ scenarios for load and irradiance. That said, for a microgrid that faces significant seasonality, many fewer daily scenarios currently drive the model's design solution. A stochastic program might yield a more robust design and further inform construction of our spinning reserve constraint. In terms of our partitioning scheme, investigating a wider range of applications may help reveal the relative merits of adaptive versus uniform partitioning. Further work could also yield insight on the advantages of alternative formulations that have weaker linear programming relaxations, but scale better with respect to the number of partitions.

Acknowledgments

The authors thank Mark Spector, Office of Naval Research, for support of this research effort under award #N000141310839. We thank Ryan Wiechens, MIT Lincoln Laboratories, and Nate Putnam, Construction Engineering Research Laboratory, for their help in

understanding the microgrid application and hardware implementation. We thank Gavin Goodall for obtaining load realizations. We thank two referees and an Associate Editor for their comments, which improved the paper.

References

A123 (2018) A123 battery manufacturer. `http://www.a123systems.com/`, accessed 2018-05-15.

Al-Khayyal FA, Falk JE (1983) Jointly constrained biconvex programming. *Mathematics of Operations Research* 8(2):273–286.

Androulakis IP, Maranas CD, Floudas CA (1995) αBB: A global optimization method for general constrained nonconvex problems. *Journal of Global Optimization* 7(4):337–363.

Bahramara S, Moghaddam MP, Haghifam M (2016) Optimal planning of hybrid renewable energy systems using HOMER: A review. *Renewable and Sustainable Energy Reviews* 62:609–620.

Baker SF, Morton DP, Rosenthal RE, Williams LM (2002) Optimizing military airlift. *Operations Research* 50(4):582–602.

Bala B, Siddiqui S (2009) Optimal design of a PV-diesel hybrid system for electrification of an isolated island in Sandwip, Bangladesh using a genetic algorithm. *Energy for Sustainable Development* 13(3):137–142.

Barbier T, Anjos M, Savard G (2014) Optimization of diesel, wind, and battery hybrid power systems. Technical Report G-2014-02, Group for Research and Decision Analysis and Department of Mathematics and Industrial Engineering Polytechnique Montréal.

Barley CD, Winn CB (1996) Optimal dispatch strategy in remote hybrid power systems. *Solar Energy* 58(4-6):165–179.

Belotti P (2009) Couenne: A user's manual. Technical report, Lehigh University, URL `https://projects.coin-or.org/Couenne/browser/trunk/Couenne/doc/couenne-user-manual.pdf?format=raw`.

Bergamini ML, Aguirre P, Grossman IE (2005) Logic-based outer approximation for globally optimal synthesis of process networks. *Computers and Chemical Engineering* 72(9):1914–1933.

Bonami P, Lee J (2009) BONMIN Version 1.4 User's Manual.

Brown GG, Dell RF, Newman AM (2004) Optimizing military capital planning. *Interfaces* 34(6):415–425.

Castro P (2015) Tightening piecewise McCormick relaxations for bilinear problems. *Computers and Chemical Engineering* 72:300–311.

Coffrin C, Hijazi H, Van Hentenryck P (2016) Network flow and copper plate relaxations for AC transmission systems. *2016 Power Systems Computation Conference (PSCC)*, 1–8 (IEEE).

Dey SS, Gupte A (2015) Analysis of MILP techniques for the pooling problem. *Operations Research* 63(2):412–427.

Dobos AP (2013) PVWatts Version 1 Technical Reference. Technical report, National Renewable Energy Laboratory.

Dolan ED, Moré JJ (2002) Benchmarking optimization software with performance profiles. *Mathematical Programming* 92(1):201–213.

Dufo-López R, Bernal-Agustín JL (2005) Design and control strategies of PV-Diesel systems using genetic algorithms. *Solar Energy* 79(1):33–46.

Dvorkin Y, Fernandez-Blanco R, Kirschen DS, Pandžić H, Watson JP, Silva-Monroy CA (2017) Ensuring profitability of energy storage. *IEEE Transactions on Power Systems* 32(1):611–623.

Erwin SI (2010) How much does the Pentagon pay for a gallon of gas? URL `http://www.nationaldefensemagazine.org/archive/2010/April/Pages/HowMuchforaGallonofGas.aspx`, accessed 2016-03-01.

Escudero LF, Garín MA, Unzueta A (2016) Cluster Lagrangean decomposition in multistage stochastic optimization. *Computers and Operations Research* 67(2016):48–62.

Felder JK, Hiskens IA (2014) Optimal power flow with storage. *Power Systems Computation Conference (PSCC), 2014*, 1–7 (IEEE).

Foy K (2018) Ten MIT Lincoln Laboratory innovations win R&D 100 awards. URL `https://www.ll.mit.edu/news/ten-mit-lincoln-laboratory-innovations-win-rd-100-awards`, accessed 2019-02-21.

Gade D, Hackebeil G, Ryan SM, Watson JP, Wets RJB, Woodruff DL (2016) Obtaining lower bounds from the progressive hedging algorithm for stochastic mixed-integer programs. *Mathematical Programming* 157:47–67.

Goodall G, Scioletti M, Zolan A, Suthar B, Newman A, Kohl P (2019) Optimal design and dispatch of a hybrid microgrid system capturing battery fade. *Optimization and Engineering* 20(1):179–213.

Gounaris CE, Misener R, Floudas CA (2009) Computational comparison of piecewise-linear relaxations for pooling problems. *Industrial & Engineering Chemistry Research* 48(12):5742–5766.

Green HJ, Manwell JF (1995) Hybrid2: A versatile model of the performance of hybrid power systems. Technical report, URL `https://www.osti.gov/scitech/servlets/purl/46678`, accessed 2017-01-11.

Gupta A, Saini R, Sharma M (2011) Modeling of hybrid energy system—Part I: Problem formulation and model development. *Renewable Energy* 36(2):459–465.

Gupte A, Ahmed S, Cheon MS, Dey S (2013) Solving mixed integer bilinear problems using MILP formulations. *SIAM Journal on Optimization* 23(2):721–744.

Hari SKK, Sundar K, Nagarajan H, Bent R, Backhaus S (2018) Hierarchical predictive control algorithms for optimal design and operation of microgrids. *Power Systems Computation Conference (PSCC), 2018* (IEEE).

Hasan M, Karimi I (2010) Piecewise linear relaxation of bilinear programs using bivariate partitioning. *AIChE Journal* 56(7):1880–1893.

Huneke F, Henkel J, González JAB, Erdmann G (2012) Optimisation of hybrid off-grid energy systems by linear programming. *Energy, Sustainability and Society* 2(1):1–19.

Husted MA, Suthar B, Goodall GH, Newman AM, Kohl PA (2018) Coordinating procurement decisions with a dispatch strategy featuring a concentration gradient. *Applied Energy* 219:394–407.

IBM (2017) CPLEX 12.6.2 User Documentation. URL `https://www.ibm.com/support/knowledgecenter/SSSA5P_12.6.2/ilog.odms.studio.help/Optimization_Studio/topics/COS_home.html`.

Karuppiah R, Grossman IE (2006) Global optimization for the synthesis of integrated water systems in chemical processes. *Computers and Chemical Engineering* 30(4):650–673.

Katsigiannis YA, Georgilakis PS (2008) Optimal sizing of small isolated hybrid power systems using tabu search. *Journal of Optoelectronics and Advanced Materials* 10(5):1241–1245.

Khodaei A, Bahramirad S, Shahidehpour M (2015) Microgrid planning under uncertainty. *IEEE Transactions on Power Systems* 30(5):2417–2425.

Lambert T, Gilman P, Lilienthal P (2005) Micropower system modeling with HOMER. Farret FA, Simões MG, eds., *Integration of Alternative Sources of Energy*, 379–418 (Wiley Online Library).

Madathil SC, Yamangil E, Nagarajan H, Barnes A, Bent R, Backhaus S, Mason SJ, Mashayekh S, Stadler M (2018) Resilient off-grid microgrids: Capacity planning and $n-1$ security. *IEEE Transactions on Smart Grid* 9(6):6511–6521.

McCormick GP (1976) Computability of global solutions to factorable nonconvex programs: Part I: Convex underestimating problems. *Mathematical Programming* 10(1):147–175.

Misener R, Thompson J, Floudas CA (2011) APOGEE: Global optimization of standard, generalized, and extended pooling problems via linear and logarithmic partitioning schemes. *Computers and Chemical Engineering* 35:876–892.

Morais H, Kádár P, Faria P, Vale ZA, Khodr HM (2010) Optimal scheduling of a renewable micro-grid in an isolated load area using mixed-integer linear programming. *Renewable Energy* 35(1):151–156.

Nagarajan H, Lu M, Wang S, Bent R, Sundar K (2019) An adaptive, multivariate partitioning algorithm for global optimization of nonconvex programs. *Journal of Global Optimization* 1–37, URL `http://dx.doi.org/10.1007/s10898-018-00734-1`.

Nagarajan H, Lu M, Yamangil E, Bent R (2016) Tightening McCormick relaxations for nonlinear programs via dynamic multivariate partitioning. *International Conference on Principles and Practice of Constraint Programming*, 369–387 (Springer).

Pruitt KA, Braun RJ, Newman AM (2013) Evaluating shortfalls in mixed-integer programming approaches for the optimal design and dispatch of distributed generation systems. *Applied Energy* 102:386–398.

Rockafellar RT, Wets RJB (1991) Scenarios and policy aggregation in optimization under uncertainty. *Mathematics of Operations Research* 16(1):119–147.

Rossum G (1995) Python reference manual. Technical report, Amsterdam, The Netherlands.

Sahinidis NV (1996) BARON: A general purpose global optimization software package. *Journal of Global Optimization* 8:201–205.

Scioletti MS (2016a) *A mixed-integer program for the design and dispatch of a hybrid power generation system*. Ph.D. thesis, Colorado School of Mines.

Scioletti MS, Goodman JK, Kohl PA, Newman AM (2016) A physics-based integer linear battery modeling paradigm. *Applied Energy* 176:245–257.

Scioletti MS, Goodman JK, Newman AM, Zolan AJ, Leyffer S (2017) Optimal design and dispatch of a system of diesel generators, photovoltaics and batteries for remote locations. *Optimization and Engineering* 18(3):755–792.

Sherali HD, Smith JC (2001) Improving discrete model representations via symmetry considerations. *Management Science* 47(10):1396–1407.

Stadler M, Groissböck M, Cardoso G, Marnay C (2014) Optimizing distributed energy resources and building retrofits with the strategic DER-CAModel. *Applied Energy* 132:557–567.

van der Kam M, van Sark W (2015) Smart charging of electric vehicles with photovoltaic power and vehicle-to-grid technology in a microgrid; a case study. *Applied Energy* 152:20–30.

Vielma JP, Ahmed S, Nemhauser G (2010a) Mixed-integer models for nonseparable piecewise-linear optimization: unifying framework and extensions. *Operations Research* 58:303–315.

Vielma JP, Nemhauser G (2010b) Modeling disjunctive constraints with a logarithmic number of binary variables and constraints. *Mathematical Programming* 128:49–72.

Wicaksono DS, Karimi IA (2008) Piecewise MILP under- and overestimators for global optimization of bilinear programs. *AIChE Journal* 54(4):991–1008.

Zhang D, Evangelisti S, Lettieri P, Papageorgiou LG (2016) Economic and environmental scheduling of smart homes with microgrid: DER operation and electrical tasks. *Energy Conversion and Management* 110:113–124.

Online Supplement
Decomposing loosely coupled mixed-integer programs for optimal microgrid design

Alexander J. Zolan
Thermal Systems Group, National Renewable Energy Laboratory, Golden, CO 80401
alexander.zolan@nrel.gov

Michael S. Scioletti
Department of Mathematical Sciences, United States Military Academy, West Point, NY 10996
michael.scioletti@usma.edu

David P. Morton
Department of Industrial Engineering and Management Sciences, Northwestern University, Evanston, IL 60208
david.morton@northwestern.edu

Alexandra M. Newman
Department of Mechanical Engineering, Colorado School of Mines, Golden, CO 80401
anewman@mines.edu

Online Supplement A. Microgrid Design and Dispatch Problem

In this Online Supplement, we describe our adaptation of the microgrid design and dispatch problem of Scioletti et al. (2017), the mapping of this detailed notation to that used in the main text, and the constraints we add to develop model ($\mathcal{P}$). The notational conventions follow those of Scioletti et al.; see their paper for more detail.

Online Supplement A.1. Full ($\mathcal{P}$) Formulation

Sets

$t \in \mathcal{T}$	time periods
$\ell \in \mathcal{L} = \{1, 2, \ldots, \lvert\mathcal{L}\rvert\}$	time blocks indexing a partition of $\mathcal{T}$; i.e., $\cup_{\ell\in\mathcal{L}}\mathcal{T}_\ell = \mathcal{T}$ and $\mathcal{T}_\ell \cap \mathcal{T}_{\ell'} = \emptyset$, $\ell \neq \ell'$
$j \in \mathcal{J}$	battery and generator technologies
$g \in \mathcal{G} \subset \mathcal{J}$	generator technologies
$b \in \mathcal{B} \subset \mathcal{J}$	battery technologies
$s \in \mathcal{S}$	PV panel types
$k \in \tilde{\mathcal{J}}_j \subset \mathcal{J}$	identical twins of technology j, given by size, type, and manufacturer
$k \in \tilde{\mathcal{G}}_g \subset \mathcal{G}$	generator twins of type g
$k \in \tilde{\mathcal{B}}_b \subset \mathcal{B}$	battery twins of type b

Timing Parameters

τ	length of one time period [hours]
υ	number of time periods per block [hours]
ν	ratio of base operation duration to time horizon length [fraction]

Optimization Model Penalty Parameters

$\tilde{c}_j$	cost of procuring one twin of technology type j [\$/twin]
c_s	cost of procuring one panel of technology type s [\$/panel]
δ_t^f	fuel cost penalty in time period t [\$/gal]
ε_j	cycle cost penalty for technology type j [\$/(hours, cycles)]

Power System Parameters

d_t^P	power demand in time period t [W]

$\bar{k}$	overage load coefficient [fraction]
k^s	spinning reserve required relative to PV power [fraction]

Technology Parameters

η_j^+, η_j^-	electric efficiency of power into and out of technology type j, respectively [fraction]
$\underline{p}_j, \bar{p}_j$	minimum and maximum power rating, respectively, of technology type j [W]

Generator Parameters

b_g^f, c_g^f	fuel consumption coefficients for generator g $[\frac{gal}{W^2h}, \frac{gal}{Wh}, \frac{gal}{h}]$

PV Parameters

γ_{st}	power output of PV technology type s in time period t, based on solar irradiance $[\frac{W}{panel}]$
$\bar{n}_s$	maximum allowable number of PV panels of technology type s [panels]

Battery Parameters

a_b^v, b_b^v	battery b voltage model coefficients [V]
d_b^{soc}, a_b^{soc}	battery b lifetime model coefficients [unitless]
b_b^0	battery b state-of-charge used in initial condition constraints [fraction]
c_b^{ref}	battery b manufacturer-specified capacity [Ah]
c_b^+, c_b^-	battery b charge and discharge capacity rate coefficients, respectively [hours]
r_b^{int}	battery b internal resistance [Ohms]
i_b^{avg}	typical current expected from battery b for both charge and discharge activities [A]
$\underline{s}_b, \bar{s}_b$	battery b state-of-charge minimum and maximum operational bounds, respectively [fraction]
i_b^{L+}, i_b^{U+}	battery b charge current lower and upper bound, respectively [A]
i_b^{L-}, i_b^{U-}	battery b discharge current lower and upper bound, respectively [A]

where, for our application, the above parameter values are computed as:

$$i_b^{L+} = 0, \quad \forall b \in \mathcal{B}$$
$$i_b^{U+} = \frac{c_b^{ref}}{c_b^+}, \quad \forall b \in \mathcal{B}.$$
$$i_b^{L-} = 0, \quad \forall b \in \mathcal{B}$$
$$i_b^{U-} = \frac{c_b^{ref}}{c_b^- + \tau}, \quad \forall b \in \mathcal{B}$$

Continuous Variables

Power Variables

P_{jkt}^+, P_{jkt}^-	aggregate power into and out of technology type j, twin k in time period t, respectively [W]
P_{st}^{PV}	aggregate power out of PV technology type s in time period t [W]

Generator Variables

$\tilde{F}_t$	amount of fuel used in time period t [gal]

Battery Variables

B_{bkt}^{soc}	state-of-charge of battery type b, twin k at end of time period t [fraction]
I_{bkt}^+, I_{bkt}^-	battery b, twin k current for charge and discharge, respectively, in time period t [A]
R	battery inventory at the beginning and end of each block [Ah]

R^ℓ battery inventory at the beginning and end of block ℓ [Ah]

Boundary Condition

$B^{soc}_{bk,0}$ initial state-of-charge of battery type b, twin k [fraction]

Binary and Integer Variables

Power Procurement Variables

W_{jk} 1 if technology j, twin k is procured, 0 otherwise

X_s integer number of PV panels of technology type s procured [panels]

W^ℓ_{jk} 1 if technology j, twin k is procured in block ℓ, 0 otherwise

X^ℓ_s integer number of PV panels of technology type s procured in block ℓ [panels]

Generator Variables

G_{gkt} 1 if technology type g, twin k is operating in time period t, 0 otherwise

Battery Variables

B^+_{bkt} 1 if battery type b, twin k is charging in time period t, 0 otherwise

B^-_{bkt} 1 if battery type b, twin k is discharging in time period t, 0 otherwise

Problem $(\mathcal{P})$

Objective Function:

Minimize

$$\frac{1}{|\mathcal{L}|}\left(\sum_{\ell\in\mathcal{L}}\sum_{j\in\mathcal{J}}\sum_{k\in\tilde{\mathcal{J}}_j}\tilde{c}_j W^\ell_{jk}+\sum_{\ell\in\mathcal{L}}\sum_{s\in\mathcal{S}}c_s X^\ell_s\right)\left(+\nu\sum_{t\in\mathcal{T}}\phi^f_t\tilde{F}_t+\nu\tau\sum_{g\in\mathcal{G}}\sum_{k\in\tilde{\mathcal{G}}_g}\sum_{t\in\mathcal{T}}\varepsilon_g G_{gkt}+\right.$$
$$\left.\nu\tau\sum_{b\in\mathcal{B}}\sum_{k\in\tilde{\mathcal{B}}_b}\sum_{t\in\mathcal{T}}\left(c_b\quad a^{soc}_b\frac{I^+_{bkt}+I^-_{bkt}}{2c^{ref}_b}-d^{soc}_b\frac{B^{soc}_{bk,t-1}I^+_{bkt}+B^{soc}_{bk,t-1}I^-_{bkt}}{2c^{ref}_b}\right)\right) \tag{14}$$

subject to

System Operations:

$$\sum_{j\in\mathcal{J}}\sum_{k\in\tilde{\mathcal{J}}_j}\left(\eta^-_j P^-_{jkt}-\sum_{b\in\mathcal{B}}\sum_{k\in\tilde{\mathcal{B}}_b}P^+_{bkt}+\sum_{s\in\mathcal{S}}P^{PV}_{st}\right)\geq(1+\bar{k})d^P_t,\ \ \forall t\in\mathcal{T} \tag{15a}$$

$$\sum_{b\in\mathcal{B}}\sum_{k\in\tilde{\mathcal{B}}_b}\left(\eta^-_b\bar{p}_b B^{soc}_{bkt}+\sum_{g\in\mathcal{G}}\sum_{k\in\tilde{\mathcal{G}}_g}\left(\bar{p}_g G_{gkt}-P^-_{gkt}\right)\right)\geq k^s\sum_{s\in\mathcal{S}}P^{PV}_{st},\ \ \forall t\in\mathcal{T} \tag{15b}$$

$$W^\ell_{j,k-1}\geq W^\ell_{jk},\ \forall j\in\mathcal{J},k\in\tilde{\mathcal{J}}_j:k>1,\ \ell\in\mathcal{L} \tag{15c}$$

Generator Operations:

$$\underline{p}_g G_{gkt}\leq P^-_{gkt}\leq\bar{p}_g G_{gkt},\ \forall g\in\mathcal{G},k\in\tilde{\mathcal{G}}_g,t\in\mathcal{T} \tag{16a}$$

$$\tilde{F}_t\geq\tau\sum_{g\in\mathcal{G}}\sum_{k\in\tilde{\mathcal{G}}_g}\left(b^f_g P^-_{gkt}+c^f_g G_{gkt}\right),\ \ \forall t\in\mathcal{T} \tag{16b}$$

$$G_{gkt}\leq W^\ell_{gk},\ \ \forall g\in\mathcal{G},k\in\tilde{\mathcal{G}}_g,t\in\mathcal{T}_\ell,\ \ell\in\mathcal{L} \tag{16c}$$

$$G_{g,k-1,t}\leq G_{gkt},\ \ \forall g\in\mathcal{G},k\in\tilde{\mathcal{G}}_g,t\in\mathcal{T}:k>1 \tag{16d}$$

$$P^-_{g,k-1,t}\leq P^-_{gkt},\ \ \forall g\in\mathcal{G},k\in\tilde{\mathcal{G}}_g,t\in\mathcal{T}:k>1 \tag{16e}$$

PV Operations:

$$P^{PV}_{st}\leq\gamma_{st}X^\ell_s,\ \ \forall s\in\mathcal{S},t\in\mathcal{T}_\ell,\ \ell\in\mathcal{L} \tag{17a}$$

$$X^\ell_s\leq\bar{n}_s,\ \ \forall s\in\mathcal{S},\ \ell\in\mathcal{L} \tag{17b}$$

Battery Operations:

$$P^+_{bkt} = a^v_b B^{soc}_{bk,t-1} I^+_{bkt} + (b^v_b + i^{avg}_b r^{int}_b) I^+_{bkt} \quad \forall b \in \mathcal{B}, k \in \tilde{\mathcal{B}}_b, t \in \mathcal{T} \tag{18a}$$

$$P^-_{bkt} = a^v_b B^{soc}_{bk,t-1} I^-_{bkt} + (b^v_b - i^{avg}_b r^{int}_b) I^-_{bkt} \quad \forall b \in \mathcal{B}, k \in \tilde{\mathcal{B}}_b, t \in \mathcal{T} \tag{18b}$$

$$B^{soc}_{bkt} = B^{soc}_{bk,t-1} + \frac{\tau(\eta^+_b I^+_{bkt} - I^-_{bkt})}{c^{ref}_b}, \quad \forall b \in \mathcal{B}, k \in \tilde{\mathcal{B}}_b, t \in \mathcal{T} \tag{18c}$$

$$\underline{s}_b W^\ell_{bk} \le B^{soc}_{bkt} \le \bar{s}_b W^\ell_{bk}, \quad \forall b \in \mathcal{B}, k \in \tilde{\mathcal{B}}_b, t \in \mathcal{T}_\ell, \ \ell \in \mathcal{L} \tag{18d}$$

$$B^{soc}_{bkt} \le B^{soc}_{b,k-1,t} + (1 - W^\ell_{bk}), \quad \forall b \in \mathcal{B}, k \in \tilde{\mathcal{B}}_b, t \in \mathcal{T}_\ell, \ell \in \mathcal{L} : k > 1 \tag{18e}$$

$$B^{soc}_{bkt} \ge B^{soc}_{b,k-1,t} - (1 - W^\ell_{bk}), \quad \forall b \in \mathcal{B}, k \in \tilde{\mathcal{B}}_b, t \in \mathcal{T}_\ell, \ell \in \mathcal{L} : k > 1 \tag{18f}$$

$$\sum_{b \in \mathcal{B}} \sum_{k \in \mathcal{B}_b} c^{ref}_b B^{soc}_{bk,(\ell-1)\cdot\upsilon} = R^\ell, \ \forall \ell \in \mathcal{L} \setminus \{1\} \tag{18g}$$

$$\sum_{b \in \mathcal{B}} \sum_{k \in \tilde{\mathcal{B}}_b} c^{ref}_b B^{soc}_{bk,\ell\cdot\upsilon} = R^\ell, \ \forall \ell \in \mathcal{L} \tag{18h}$$

$$\underline{p}_b B^+_{bkt} \le P^+_{bkt} \le \bar{p}_b B^+_{bkt}, \ \forall b \in \mathcal{B}, k \in \tilde{\mathcal{B}}_b, t \in \mathcal{T} \tag{18i}$$

$$\underline{p}_b B^-_{bkt} \le P^-_{bkt} \le \bar{p}_b B^-_{bkt}, \ \forall b \in \mathcal{B}, k \in \tilde{\mathcal{B}}_b, t \in \mathcal{T} \tag{18j}$$

$$i^{L+}_b B^+_{bkt} \le I^+_{bkt} \le i^{U+}_b B^+_{bkt}, \quad \forall b \in \mathcal{B}, k \in \tilde{\mathcal{B}}_b, t \in \mathcal{T} \tag{18k}$$

$$i^{L-}_b B^-_{bkt} \le I^-_{bkt} \le i^{U-}_b B^-_{bkt}, \quad \forall b \in \mathcal{B}, k \in \tilde{\mathcal{B}}_b, t \in \mathcal{T} \tag{18l}$$

$$I^-_{bkt} \le i^{U-}_b B^{soc}_{bk,t-1}, \quad \forall b \in \mathcal{B}, k \in \tilde{\mathcal{B}}_b, t \in \mathcal{T} \tag{18m}$$

$$B^+_{bkt} + B^-_{bkt} \le W^\ell_{bk}, \quad \forall b \in \mathcal{B}, k \in \tilde{\mathcal{B}}_b, t \in \mathcal{T}_\ell, \ell \in \mathcal{L} \tag{18n}$$

$$B^+_{bkt} + B^-_{b'k't} \le 1, \quad \forall b, b' \in \mathcal{B}; k, k' \in \tilde{\mathcal{B}}_b; t \in \mathcal{T} : b \ne b', k \ne k' \tag{18o}$$

Nonanticipativity:

$$W^\ell_{jk} = W_{jk}, \ \forall j \in \mathcal{J}, k \in \tilde{\mathcal{J}}_j, \ell \in \mathcal{L} \tag{19a}$$

$$X^\ell_s = X_s, \ \forall s \in \mathcal{S}, \ell \in \mathcal{L} \tag{19b}$$

$$R^\ell = R, \ \forall \ell \in \mathcal{L} \setminus \{1\} \tag{19c}$$

Boundary Condition:

$$B^{soc}_{bk,0} = b^0_b W_{bk}, \quad \forall b \in B, k \in \tilde{\mathcal{B}}_b \tag{20}$$

Nonnegativity and Integrality:

$$P^+_{jkt}, P^-_{jkt} \ge 0, \quad \forall j \in \mathcal{J}, k \in \tilde{\mathcal{J}}_j, t \in \mathcal{T} \tag{21a}$$

$$P^{PV}_{st} \ge 0, \quad \forall s \in \mathcal{S}, t \in \mathcal{T} \tag{21b}$$

$$\tilde{F}_t \ge 0, \quad t \in \mathcal{T} \tag{21c}$$

$$B^{soc}_{bkt}, I^+_{bkt}, I^-_{bkt} \ge 0, \quad \forall b \in \mathcal{B}, k \in \tilde{\mathcal{B}}_b, t \in \mathcal{T} \tag{21d}$$

$$R \quad \text{unrestricted} \tag{21e}$$

$$R^\ell \quad \text{unrestricted}, \quad \forall \ell \in \mathcal{L} \tag{21f}$$

$$B^{soc}_{bk,0} \ge 0, \quad \forall b \in \mathcal{B}, k \in \tilde{\mathcal{B}}_b \tag{21g}$$

$$W_{jk} \in \{0,1\}, \quad \forall j \in \mathcal{J}, k \in \tilde{\mathcal{J}}_j \tag{21h}$$

$$X_s \in \mathbb{Z}^+, \quad \forall s \in \mathcal{S} \tag{21i}$$

$$W^{\ell}_{jk} \in \{0,1\}, \quad \forall j \in \mathcal{J}, k \in \tilde{\mathcal{J}}_j, \ell \in \mathcal{L} \tag{21j}$$

$$X^{\ell}_s \in \mathbb{Z}^+, \quad \forall s \in \mathcal{S}, \ell \in \mathcal{L} \tag{21k}$$

$$G_{gkt} \in \{0,1\}, \quad \forall g \in \mathcal{G}, k \in \tilde{\mathcal{G}}_g, t \in \mathcal{T} \tag{21l}$$

$$B^{+}_{bkt}, B^{-}_{bkt} \in \{0,1\}, \quad \forall b \in \mathcal{B}, k \in \tilde{\mathcal{B}}_b, t \in \mathcal{T} \tag{21m}$$

Discussion

Online Supplement A.1.1. Objective function. We minimize the objective function in (14), which includes the cost of (i) procuring diesel generators, batteries and PV systems, (ii) consuming fuel, and (iii) using the technologies in dispatch, measured in lifecycles; a generator uses one lifecycle for each hour it is running, while a battery uses lifecycles according to a function of the charge current and state-of-charge of the battery in each time period. We assume that the fixed costs associated with procurement of the generators, batteries, and PV systems account for the operating horizon of the FOB, i.e., each such cost is the difference in value between a new technology and its salvage value after the deployment is complete. Our implementation of lifecycle costs is analogous to assigning values to variable L_{jk} via constraints (6a) and (14) from Scioletti et al. (2017); however, we do not impose a restriction on the number of lifecycles spent per constraint (6c) from their paper. The parameter ν reconciles the time horizon of the optimization model with that of the FOB's duration.

Online Supplement A.1.2. System operations. Constraint (15a) requires that the dispatch strategy meets demand for each hour; the efficiency parameter, η^{-}_j, denotes the (fixed) efficiency losses applied to battery power output that supplement those that we describe in Section 3.3. Constraint (15b) enforces a spinning reserve requirement that is equal to a fraction of PV power output in each time period. Alternative approaches model spinning reserve requirements as a function of the demand not met by PV systems (see, e.g., Husted et al. 2018). Constraint (15c) breaks symmetry (Sherali and Smith 2001). Our model adopts the "copper plate" model discussed in Coffrin et al. (2016), which does not include power flow constraints. Rather, we assume that power supply must meet load in each time period without regard for line-specific losses or transmission capacity constraints; this assumption is reasonable for the size of microgrid we consider.

Online Supplement A.1.3. Generator operations. Constraint (16a) restricts power output of generators to their specific minimum and maximum power ratings. Constraint (16b) determines fuel consumption as a function of whether each generator in the microgrid design is running, and, if so, its power output. While Scioletti et al. (2017) include a second-order term in the relationship, i.e.,

$$\tilde{F}_t \geq \tau \sum_{g \in \mathcal{G}} \sum_{k \in \tilde{\mathcal{G}}_g} \Big(a^f_g (P^{-}_{gkt})^2 + b^f_g P^{-}_{gkt} + c^f_g G_{gkt} \Big), \quad \forall t \in \mathcal{T},$$

their implementation sets the value of the parameter a^f_g to zero. Constraint (16c) connects procurement to dispatch, and constraints (16d) and (16e) break symmetry.

Online Supplement A.1.4. PV operations. Constraint (17a) enforces an upper bound on PV output power per panel according to the solar irradiance in each hour. Constraint (17b) limits the number of systems in the design according to spatial restrictions.

Online Supplement A.1.5. Battery operations. Constraints (18a) and (18b) restrict the net power output of the battery to the product of the battery's voltage and its net current for each time period; this is consistent with the battery modeling paradigm developed by Scioletti et al. (2016). Our implementation does not use a decision variable for voltage, but rather, uses the right-hand side of constraint (5g) from Scioletti et al. (2017) to model battery voltage. While the implementation from Scioletti et al. includes the products of terms $B^{+}_{bk,t-1} \cdot I^{+}_{bkt}$ and $B^{-}_{bk,t-1} \cdot I^{-}_{bkt}$ on the right-hand sides of constraints (18a) and (18b), respectively, the bounds provided in constraints (18k)-(18l) require that $I^{+}_{bkt} = 0$ when the battery is not charging, and that $I^{-}_{bkt} = 0$ when the battery is not discharging, i.e., $B^{+}_{bkt} \cdot I^{+}_{bkt} = I^{+}_{bkt}$ and $B^{-}_{bkt} \cdot I^{-}_{bkt} = I^{-}_{bkt}$. As a result, our constraints (18a)-(18b) are an equivalent formulation to constraints (5a), (5b), and (5g) from the predecessor paper.

Constraint (18c) updates the battery state-of-charge according to charge and discharge currents, the former of which is modified by an efficiency term, η^{+}_{b}. Constraint (18d) enforces upper and lower bounds on the battery's state-of-charge. Constraints (18e) and (18f) force all batteries in the design to maintain the same state-of-charge. Constraints (18g)-(18h) enforce the reset policy described in Section 2.1. Constraints (18i) and (18j) provide upper and lower bounds for net power, while constraints (18k) through (18m) provide similar bounds for net current. Constraints (18n) and (18o) preclude simultaneous charging and discharging of batteries.

Online Supplement A.1.6. Nonanticipativity and boundary condition. Constraints (19) require a single design and reset inventory level. In the lower bound model, ($\underline{\mathcal{P}}$), we implement a Lagrangian relaxation of these constraints with multipliers that we update via Algorithm 1. In the upper bound model, ($\bar{\mathcal{P}}$), we provide (fixed) values for: $W_{bk}, \forall b \in \mathcal{B},\ k \in \tilde{\mathcal{B}}_b$; $X_s, \forall s \in \mathcal{S}$; and, R. Constraint (20) enforces a specific initial state-of-charge for each battery in the design.

Online Supplement A.1.7. Nonnegativity and integer restrictions. Constraints (21) provide nonnegativity and integer restrictions for the design and dispatch decision variables. Our implementation relaxes constraint (21i) to allow fractional values for $X^{\ell}_{s},\ \forall s \in \mathcal{S},\ \ell \in \mathcal{L}$.

Online Supplement A.2. Mapping Microgrid Design and Dispatch Problem to Model ($\mathcal{P}$)

We map the technology purchase decision variables, $W_{jk},\ j \in \mathcal{J}, k \in \tilde{\mathcal{J}}_j$, and $X_s,\ s \in \mathcal{S}$, to the decision vector X in model ($\mathcal{P}$), and variable R in the detailed model of this Online Supplement maps directly to R in model ($\mathcal{P}$). We map $B^{soc}_{bk,t-1}$ and $B^{soc}_{bkt},\ b \in \mathcal{B}, k \in \tilde{\mathcal{B}}_b$, to $\underline{Y}_t$ and $\bar{Y}_t$, respectively, in model ($\mathcal{P}$) for all $t \in \mathcal{T}$. We map all other decision variables to $Y_t,\ t \in \mathcal{T}$. Focusing on model (9)'s reformulation of model ($\mathcal{P}$), constraints (15c), (17b), and (21h)-(21k) correspond to constraint (9b). Constraint (18c) corresponds to constraints (9d)-(9e), which are condensed by substituting the variable for each battery's starting state-of-charge in period t with that of its ending state-of-charge at period $t-1$. Constraints (18g)-(18h) correspond

to constraints (9f)-(9g). Nonanticipativity constraints (19) correspond to constraints (9h) and (9i), and the boundary condition (20) corresponds to constraint (9j). All other constraints constitute (9c) in model $(\mathcal{P})$. We model the inventory variables $\bar{Y}_t$ as total battery capacity via:

$$\bar{Y}_t = \sum_{b\in\mathcal{B}} \sum_{k\in\tilde{\mathcal{B}}_b} \left(\epsilon_b^{ref} B_{bkt}^{soc}, \ \forall t \in \mathcal{T}, \right. \tag{22}$$

and calculate $\underline{Y}_t$ and R similarly. This allows us to use a single value for R when we perform the bisection search in Algorithm 1.

Online Supplement A.3. Mapping Linearization to Model $(\mathcal{U})$

Because voltage is a function of battery state-of-charge, we substitute the products $B_{bk,t-1}^{soc} \cdot I_{bkt}^{+}$ and $B_{bk,t-1}^{soc} \cdot I_{bkt}^{-}$ with the linearization variables Z_{bkt}^{+} and Z_{bkt}^{-}, respectively, and constraints (23) and (24) enforce the bilinear relationships in the nonlinear model $(\mathcal{P})$:

$$Z_{bkt}^{+} = B_{bk,t-1}^{soc} I_{bkt}^{+}, \quad \forall b \in \mathcal{B}, k \in \tilde{\mathcal{B}}_b, t \in \mathcal{T} \tag{23}$$

$$Z_{bkt}^{-} = B_{bk,t-1}^{soc} I_{bkt}^{-}, \ \ \forall b \in \mathcal{B}, k \in \tilde{\mathcal{B}}_b, t \in \mathcal{T}. \tag{24}$$

We map the state-of-charge variables, $B_{bk,t-1}^{soc}$, and current variables, I_{bkt}^{+}, to Y_{1t} and Y_{2t}, respectively, for each battery, twin and time period; we perform an analogous mapping for B_{bkt}^{soc} and I_{bkt}^{-}. Rather than just having a simple lower bound, variable I_{bkt}^{+} has a lower bound of i_b^{L+} if binary variable B_{bkt}^{+} is one and otherwise the lower bound is zero, with an analogous bound of i_b^{L-} for I_{bkt}^{-} if $B_{bkt}^{-} = 1$ and zero otherwise; see constraints (18k)-(18l). Likewise, variable B_{bkt}^{soc} has a lower bound of $\underline{s}_b$ if $W_{bk}^{\ell} = 1$, and zero otherwise. The following variant of constraints (8) incorporates these restrictions using binary variables B_{bkt}^{+}, B_{bkt}^{-}, and W_{bk}^{ℓ}:

Sets

$n \in \mathcal{N}$	set of all subregions in partitioning of support of current

New Battery Parameters

i_{bn}^{L+}	minimum charge current to battery b in subregion n (A)
i_{bn}^{U+}	maximum charge current to battery b in subregion n (A)
i_{bn}^{L-}	minimum discharge current from battery b in subregion n (A)
i_{bn}^{U-}	maximum discharge current from battery b in subregion n (A)

New Battery Variables

Z_{bkt}^{+}, Z_{bkt}^{-}	battery b, twin k auxiliary variable for product, and charge and discharge current, respectively, and starting state-of-charge in period t [A]
λ_{bknt}^{+}	1 if charge current for battery b, twin k is in subregion n at period t, 0 otherwise
λ_{bknt}^{-}	1 if discharge current for battery b, twin k is in subregion n at period t, 0 otherwise

Constraints

$$\sum_{n\in\mathcal{N}} \left(\lambda_{bknt}^{+} = B_{bkt}^{+}, \ \ \forall b \in \mathcal{B}, k \in \tilde{\mathcal{B}}_b, t \in \mathcal{T} \right. \tag{25a}$$

$$\sum_{n\in\mathcal{N}} \left(\lambda_{bknt}^{-} = B_{bkt}^{-}, \ \ \forall b \in \mathcal{B}, k \in \tilde{\mathcal{B}}_b, t \in \mathcal{T} \right. \tag{25b}$$

$$I^+_{bkt} \geq i^{L+}_b B^+_{bkt} + (i^{L+}_{bn} - i^{L+}_b)\lambda^+_{bknt}, \quad \forall b \in \mathcal{B}, k \in \tilde{\mathcal{B}}_b, n \in \mathcal{N}, t \in \mathcal{T} \tag{25c}$$

$$I^+_{bkt} \leq i^{U+}_b B^+_{bkt} - (i^{U+}_b - i^{U+}_{bn})\lambda^+_{bknt}, \quad \forall b \in \mathcal{B}, k \in \tilde{\mathcal{B}}_b, n \in \mathcal{N}, t \in \mathcal{T} \tag{25d}$$

$$I^-_{bkt} \geq i^{L-}_b B^-_{bkt} + (i^{L-}_{bn} - i^{L-}_b)\lambda^-_{bknt}, \quad \forall b \in \mathcal{B}, k \in \tilde{\mathcal{B}}_b, n \in \mathcal{N}, t \in \mathcal{T} \tag{25e}$$

$$I^-_{bkt} \leq i^{U-}_b B^-_{bkt} - (i^{U-}_b - i^{U-}_{bn})\lambda^-_{bknt}, \quad \forall b \in \mathcal{B}, k \in \tilde{\mathcal{B}}_b, n \in \mathcal{N}, t \in \mathcal{T} \tag{25f}$$

$$Z^+_{bkt} \geq i^{U+}_{bn} B^{soc}_{bk,t-1} + \bar{s}_b I^+_{bkt} - \bar{s}_b i^{U+}_{bn} W^\ell_{bk} - (\bar{s}_b - \underline{s}_b)(i^{U+}_b - i^{U+}_{bn})(W^\ell_{bk} - \lambda^+_{bknt}),$$
$$\forall b \in \mathcal{B}, k \in \tilde{\mathcal{B}}_b, n \in \mathcal{N}, t \in \mathcal{T}_\ell, \ell \in \mathcal{L} \tag{25g}$$

$$Z^+_{bkt} \geq i^{L+}_{bn} B^{soc}_{bk,t-1} + \underline{s}_b I^+_{bkt} - \underline{s}_b i^{L+}_{bn} W^\ell_{bk} - (\bar{s}_b - \underline{s}_b)(i^{L+}_{bn} - i^{L+}_b)(W^\ell_{bk} - \lambda^+_{bknt}),$$
$$\forall b \in \mathcal{B}, k \in \tilde{\mathcal{B}}_b, n \in \mathcal{N}, t \in \mathcal{T}_\ell, \ell \in \mathcal{L} \tag{25h}$$

$$Z^+_{bkt} \leq i^{L+}_{bn} B^{soc}_{bk,t-1} + \bar{s}_b I^+_{bkt} - \bar{s}_b i^{L+}_{bn} W^\ell_{bk} + (\bar{s}_b - \underline{s}_b)(i^{L+}_{bn} - i^{L+}_b)(W^\ell_{bk} - \lambda^+_{bknt}),$$
$$\forall b \in \mathcal{B}, k \in \tilde{\mathcal{B}}_b, n \in \mathcal{N}, t \in \mathcal{T}_\ell, \ell \in \mathcal{L} \tag{25i}$$

$$Z^+_{bkt} \leq i^{U+}_{bn} B^{soc}_{bk,t-1} + \underline{s}_b I^+_{bkt} - \underline{s}_b i^{U+}_{bn} W^\ell_{bk} + (\bar{s}_b - \underline{s}_b)(i^{U+}_b - i^{U+}_{bn})(W^\ell_{bk} - \lambda^+_{bknt}),$$
$$\forall b \in \mathcal{B}, k \in \tilde{\mathcal{B}}_b, n \in \mathcal{N}, t \in \mathcal{T}_\ell, \ell \in \mathcal{L} \tag{25j}$$

$$Z^-_{bkt} \geq i^{U-}_{bn} B^{soc}_{bk,t-1} + \bar{s}_b I^-_{bkt} - \bar{s}_b i^{U-}_{bn} W^\ell_{bk} - (\bar{s}_b - \underline{s}_b)(i^{U-}_b - i^{U-}_{bn})(W^\ell_{bk} - \lambda^-_{bknt}),$$
$$\forall b \in \mathcal{B}, k \in \tilde{\mathcal{B}}_b, n \in \mathcal{N}, t \in \mathcal{T}_\ell, \ell \in \mathcal{L} \tag{25k}$$

$$Z^-_{bkt} \geq i^{L-}_{bn} B^{soc}_{bk,t-1} + \underline{s}_b I^-_{bkt} - \underline{s}_b i^{L-}_{bn} W^\ell_{bk} - (\bar{s}_b - \underline{s}_b)(i^{L-}_{bn} - i^{L-}_b)(W^\ell_{bk} - \lambda^-_{bknt}),$$
$$\forall b \in \mathcal{B}, k \in \tilde{\mathcal{B}}_b, n \in \mathcal{N}, t \in \mathcal{T}_\ell, \ell \in \mathcal{L} \tag{25l}$$

$$Z^-_{bkt} \leq i^{L-}_{bn} B^{soc}_{bk,t-1} + \bar{s}_b I^-_{bkt} - \bar{s}_b i^{L-}_{bn} W^\ell_{bk} + (\bar{s}_b - \underline{s}_b)(i^{L-}_{bn} - i^{L-}_b)(W^\ell_{bk} - \lambda^-_{bknt}),$$
$$\forall b \in \mathcal{B}, k \in \tilde{\mathcal{B}}_b, n \in \mathcal{N}, t \in \mathcal{T}_\ell, \ell \in \mathcal{L} \tag{25m}$$

$$Z^-_{bkt} \leq i^{U-}_{bn} B^{soc}_{bk,t-1} + \underline{s}_b I^-_{bkt} - \underline{s}_b i^{U-}_{bn} W^\ell_{bk} + (\bar{s}_b - \underline{s}_b)(i^{U-}_b - i^{U-}_{bn})(W^\ell_{bk} - \lambda^-_{bknt}),$$
$$\forall b \in \mathcal{B}, k \in \tilde{\mathcal{B}}_b, n \in \mathcal{N}, t \in \mathcal{T}_\ell, \ell \in \mathcal{L} \tag{25n}$$

$$Z^+_{bkt} \leq \bar{s}_b I^+_{bkt}, \quad \forall b \in \mathcal{B}, k \in \tilde{\mathcal{B}}_b, t \in \mathcal{T} \tag{25o}$$

$$Z^-_{bkt} \leq \bar{s}_b I^-_{bkt}, \quad \forall b \in \mathcal{B}, k \in \tilde{\mathcal{B}}_b, t \in \mathcal{T} \tag{25p}$$

$$\lambda^-_{bknt}, \lambda^+_{bknt} \in \{0,1\}, \quad \forall b \in \mathcal{B}, k \in \tilde{\mathcal{B}}_b, n \in \mathcal{N}, t \in \mathcal{T} \tag{25q}$$

$$Z^+_{bkt}, Z^-_{bkt} \geq 0, \quad \forall b \in \mathcal{B}, k \in \tilde{\mathcal{B}}_b, t \in \mathcal{T}. \tag{25r}$$

Constraints (25a)-(25n) replicate the linearization constraints (8) applied to the microgrid design and dispatch problem for each battery technology and twin. Constraints (25o)-(25p) require that $Z^+_{bkt} = 0$ when battery b, twin k is not charging in period t, and that $Z^-_{bkt} = 0$ when the battery is not discharging, respectively.

Online Supplement B. Repository of Data and Code

Data and code are available in a GitHub repository: `https://github.com/zolanaj/RemoteMicrogridOpt`.